POLITECNICO DI MILANO

School of Industrial and Information Engineering

Department of Chemistry, Materials and Chemical Engineering
"Giulio Natta"

Master of Science in Chemical Engineering

Study of the kinetic model and plant steady-state simulation for the synthesis of methanol from syngas on a synthetic Cu/ZnO/Al$_2$O$_3$ catalyst

Supervisor:
Prof.Dott.Ing. Flavio MANENTI

Candidate:
Paolo Francesco RIVA RIQUELME
Matr. n. 897150

Academic Year 2017-2019

This work is dedicated to my parents. Who encouraged me to achieve my final form.

To my brother and sisters for sending me pictures of my pets while studying abroad.

To my polola and friends here in Milan, without whom I probably would have become a hermit by now.

And to my friends in Chile, who still don't get bored of having a long distance friendship.

"Everything looks smarter as a quote
(u/I_am_unique6435, 2019)

Contents

List of Figures

List of Tables

List of Symbols and Acronyms

Symbols

c_s Free active sites

c_t Total number of sites

f_i Fugacity of component i

K_i^{eq} Chemical equilibrium coefficient of reaction i

P Pressure

P_i Partial pressure of component i

T Temperature

Z Compressibility factor

Acronyms

CAPEX   Capital expenditures

CCS   Carbon capture and storage

CCU   Carbon capture units

CZA   Copper-Zinc-Aluminum

DME   Dimethyl ether

DMFC   Direct methanol fuel cell

EoS   Equation of state

GHG   Greenhouse gases

GHSV   Gas hourly space velocity

MeOH   Methanol

OPEX   Operating expenditures

PEMFC   Proton exchange membrane fuel cell

PV   Photovoltaic

RDS   Rate determining step

RWGS   Reverse water gas shift

SRK   Soave-Redlich-Kwong

SV   Space velocity

WGS   Water gas shift

Abstract

The kinetic of low-pressure methanol synthesis study was performed on a synthetic CZA catalyst by undergoing a reparametrization process for three renowned kinetic models; Vanden Bussche, Graaf, Park. From the results, Vanden Bussche's model with custom parameters showed the best representation of the kinetics involved. Later, this customized model was employed to simulate a plug flow reactor to which a sensitivity analysis was applied. The results were clear, is crucial to choose a configuration that forces the WGS reaction to occur in the forward direction, and by this, setting the CO_2 hydrogenation as the consecutive reaction; this way the WGS reaction will produce the CO_2 needed for the hydrogenation reaction while simultaneously consuming the water produced by it. The best configuration for maximizing the methanol production in a standalone reactor was establish. As methanol synthesis is recognizable by having low conversion per pass, which makes it compulsory the use of a recycle stream in plant application, a steady state plant simulation was performed with the custom kinetic model in its core. The results showed that methanol production can be maximized for a plant feed with CO ratio = 0.95, S = 1.9; which reaches a value of 0.71 and 2.64 respectively at the reactor's inlet. Under this configuration, for a plant's feed of 1500 kgmol/h a methanol production of 15100 kg/h is achieved while maintaining a low molar recycle ratio of 4.2.

Estratto

La cinetica dello studio di sintesi del metanolo a bassa pressione è stata eseguita su un catalizzatore CZA sintetico sottoposti a un proceso di reparametrizzazione per tre rinomati modelli cinetici; Vanden Bussche, Graaf, Park. Dai risultati, il modello di Vanden Bussche con parametri personalizzati ha mostrato la migliore rapprasentazione delle cinetiche coinvolte. Successivamente, questo modello personalizzato è stato impiegato per simulare un reattore con flusso a pistone al quale è stata applicata un'analisi di sensibilità. I risultati sono stati chiari, è fondamentale scegliere una configurazione che costringa la reazione WGS ad avvenire nella direzione avanti, e da questo, impostando l'idrogenazione di CO_2 come reazione consecutiva; in questo modo la reazione WGS produrrà la CO_2 necessaria per la reazione di idrogenazione consumando contemporaneamente l'acqua prodotta da essa. È stata stabilita la configurazione per massimizzare la produzione di metanolo per un reatore a sé stante. Paiché la sintesi di metanolo è riconoscibile avendo una bassa conversione per passaggio, il che rende obbligatorio l'uso di un flusso di riciclo nell'applicazione dell'impianto, è stata eseguita una simulazione di impianto allo stato stazionario utilizzando il modelo cinetico personalizzato. I risultati hanno mostrato che la produzione di metanolo può essere massimizzata per una alimentazione allo impianto con CO ratio = 0.95, S = 1.9; che raggiunge un valore di 0.71 e 2.64 rispettivamente all'ingresso del reatore. In questa configurazione, per un impianto con una alimentazione di 1500 kgmol/h si ottiene una produzione di metanolo di 15100 kg/h mantenendo un basso rapporto di ricicle molare uguale a 4.2.

Parole Chiave   metanolo; cinetica; modelo cinetico; parametrizzazione; simulazioni di processi allo stato stazionario

Chapter 1:
Context

Global warming and climate change are both one of the biggest and more challenging problems of the 21st century, they are caused by the increasing release of greenhouse gases (GHG), among them, carbon dioxide (CO_2) is the specie that makes the most contribution to this effect. The emission of CO_2 is mainly related to the combustion of fossil fuels to satisfy the world energy demands which is expected to keep increasing along the following years. Because of this, science has been focused on studying alternative energy sources that allow a reduction on the net CO_2 emission. Renewable energy sources allow to satisfy part of the energy demand without contributing to the greenhouse effect, however, today most of energy sources are still implicated on the production of CO_2.

The most common type of the world's renewable generation capacity by energy sources is hydropower (50%), Wind (24%), and Solar PV (20%) (*Data and Statistics - IRENA REsource*). All of them share the same predicament of being intermittency, which makes it difficult to satisfy the energy demand at all hours without the support of non-renewable energy sources to fill the "gap". An interesting approach to resolve the intermittency problem is the use of energy storage technologies, from which, the only realistic alternative is the energy storage in chemical bonds for further energy release by combustion or fuel cells utilization at energy demanding times.

Methanol (octane number of 113) is an interesting chemical compound for this purpose, it is liquid at room temperature and pressure which makes it easy to transport, it can store more potential energy per volume than liquified hydrogen (Shamsul *et al.*, 2014). It can be used in fuel cells in direct methanol fuel cell (DMFC), technology under a rapid development thanks to its low pollution, fast operation, high energy density and structural simplicity by being able to produce electricity without a reformer or humidifier (Lu, Liu and Wang, 2005; Wee, 2007).

It can be synthetized from syngas, a fuel gas mixture consisting primarily of hydrogen, carbon monoxide and very often carbon dioxide. Catalytic conversion of CO_x to methanol is acknowledged as a promising process that might offer a comprehensive solution to the issues of greenhouse gas control and depletion of fossil fuels. Methanol is a significant starting product for a number of valuable chemicals, it can be converted into aromatics, ethylene, and propylene as well as to other value-added petrochemicals that are nowadays mainly derived from crude oil (Aresta, Dibenedetto and Angelini, 2013). Moreover, methanol was mainly applied as a starting feedstock in the chemical industries and it could be an efficient sustainable and alternative synthetic fuel if anthropogenic CO_x and regenerative H_2 are used as reagent for its synthesis. One of the current tasks to optimize this process is to explore high selective and active catalysts.

Carbon Capture and Storage (CCS) units can capture up to 90% of the carbon dioxide emissions produced from the combustion of fossil fuels in industrial processes, preventing the carbon

dioxide from entering the atmosphere by storage it or by recycling it as a raw material. And electrolysis is a promising alternative for hydrogen production from renewable resources by using electricity to split water into hydrogen and oxygen. This way maintaining a complete renewable process.

Chapter 2:

Methanol Synthesis

In this chapter we will focus on the synthesis of methanol from syngas (a mixture of H_2, CO and CO_2) over a $Cu/ZnO/Al_2O_3$ (CZA) catalysts. Giving special emphasis at the evolution of the technologies implicated and their relationship to the maturity on the understanding of the kinetic involved.

2.1   State of the Art

Methanol synthesis is industrially carried out through catalytic conversion of syngas. The production process consists of three main reactions: CO hydrogenation (Eq. 2.1), water gas shift reaction (Eq. 2.2), and CO_2 hydrogenation (Eq. 2.3).

 i.   CO hydrogenation:

$$CO + 2H_2 \rightleftarrows CH_3OH; \quad \Delta H^o_{298K} = -90.8 \ [kJ/mol]$$
<div align="right">*Eq. 2.1*</div>

 ii.   Water gas shift reaction:

$$CO + H_2O \rightleftarrows CO_2 + H_2; \quad \Delta H^o_{298K} = -41.17 \ [kJ/mol]$$
<div align="right">*Eq. 2.2*</div>

 iii. CO_2 hydrogenation:

$$CO_2 + 3H_2 \rightleftarrows CH_3OH + H_2O; \quad \Delta H^o_{298K} = -49.2 \ [kJ/mol]$$
<div align="right">*Eq. 2.3*</div>
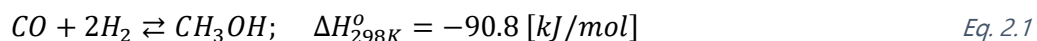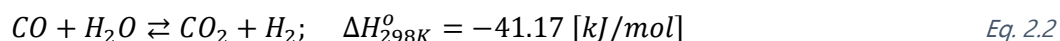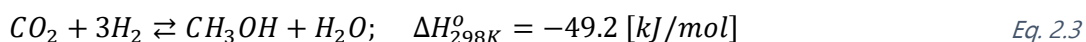
As presented on the reactions above, the synthesis of methanol is an exothermic process affected by thermodynamic equilibrium with an overall reduction on moles; for this reason, the process is favored at low temperatures and at high pressures (Dybkjær *et al.*, 2006). Under normal synthesis conditions (7.5 MPa, 225 °C), carbon conversion in traditional gas reactors cannot overcome the thermodynamic limit around 60% (Dybkjær *et al.*, 2006).

Converting one mole of CO_2 to methanol requires an energy input around 228 kJ and six electrons to reduce C^{4+} of carbon dioxide into C^{2-} of methanol. The carbon-oxygen bonds are very strong, therefore high energy is required to break them. Because of this, a good catalytic system is required. The transformation of CO_2, a greenhouse gas, into a more useful and demanding commodity is a practical approach to sustainable development (Liu *et al.*, 2003). Under this conception, CO_2 can be captured by Carbon Capture Units (CCU) from any natural or industrial source. With regard to hydrogen, it can be obtained from water dissociation by electrolysis (Eq. 2.4) using a renewable source of electricity. By this, it is possible to use methanol to store renewable energy on a large, long-term, easily transportable and storable way (Ganesh, 2014).

$$2H_2O \longrightarrow 2H_2 + O_2$$
<div align="right">*Eq. 2.4*</div>

The composition of the syngas is usually characterized by the stoichiometric number S (Eq. 2.5).

$$S = \frac{moles\ H_2 - moles\ CO_2}{moles\ CO_2 + moles\ CO}$$

The value of S depends on the adopted raw materials. When syngas is produced by means of natural gas reforming an S value of $2.8 - 3.0$ is usually archived.

The methanol synthesis process should contain a small proportion of inert gases, studies have shown an optimal $H_2:CO_2$ molar ratio in the syngas >2 (Specht and Bandi, 1999). The water gas shift process is the most frequently used to ensure a suitable ratio of $CO_2:CO:H_2$ and mainly to convert CO into CO_2.

In addition, the conversion of synthesis gas is subjected to a thermodynamic equilibrium that limits the process to a low conversion per pass, therefore, a large recycle of unconverted gas should ne taken into account. The resulting recycle and cooling duty are largely responsible for the operative cost of the plant.

A thorough experimental evaluation of the chemical equilibrium in CO hydrogenation (Eq. 2.1) and water gas shift reaction (Eq. 2.2) was done by Graaf (Graaf *et al.*, 1986), the authors studied a fixed-bed catalytic reactor at a pressure range of $10 - 80$ bar and a temperature range of $200 - 270$ °C and described the equilibrium as being the result of ideal gas behavior, but after, it was corrected for nonideality of the gas mixture using the Soave-Redlich-Kwong equation of state (Soave, 1972).

There is plenty of benefits in using CO_2 as a precursor to other chemicals; it is remarkably cheap, as it is taxed by governments if released to the atmosphere as a global warming regulation, being a subproduct of combustion processes, it is hugely available worldwide (Effective Carbon Rates 2018, 2018). Chemically, CO_2 is a non-toxic, non-corrosive, non-inflammable compound that can be easily transported on pipes as gas or in liquid form under moderate pressure and processed in existing methanol synthesis from syngas plants without significant alteration (Centi and Perathoner, 2009).

Methanol synthesis in situ allows the elusion of expensive CO_2 sequestration and offers a cheaper and economically attractive alternative reducing the global warming impact by reducing the release of greenhouse gases to the atmosphere (Olah, 2005; Tanaka, 2008).

Methanol is involved in another technology that has begun gaining attention in the last years; fuel cells. Their main advantage of direct methanol fuel cells (DMFC) over the more common proton exchange membrane fuel cells (PEMFC) is the ease of transportation and storage, higher energy density, the elimination of fuel reformer and humidifiers, and reasonably stable liquid at all environmental conditions (Lamy *et al.*, 2002; Qian *et al.*, 2006; Demirci, 2007; Li and Faghri, 2013).

It is thought that methanol and dimethyl ether will replace fossil fuels as a mean of energy storage, ground transportation fuel, and raw material for synthetic hydrocarbon and their products; concept referred as methanol economy (Gumber and Gurumoorthy, 2018).

2.2   Processes and Technologies

Methanol production processes have endured through a constant shift over the years as a consequence of breakthroughs around the science surrounding the matter and by the change of the world commodities availabilities and purities. A brief description of the key process of methanol synthesis is presented at continuation.

2.2.1   The BASF process – high pressure method

On 1923, A. Mittasch and M. Pier discovered the hydrogenation of carbon monoxide with an iron-based catalyst at 500 °C and 100 bar operation while studying the ammonia metal-catalyzed synthesis (Mittasch and Pier, 1925). The process presented low yield because of pollutants presence on the reactant gases: chlorine, hydrogen sulfide, methane, and other hydrocarbons; which caused the deactivation of the iron catalyst. Since then, a great variety of oxides and metals have been tested as hydrogenation catalysts with all reactions being conducted at high pressure, 250 – 300 bar, and high temperature, 320 – 450 °C. Among all the experiments, there were two catalysts that gave the best results under these conditions: ZnO/Cr_2O_3 and ZnO/CuO (Marek and Hahn, 1933; Kung, 1980).

Out of these results, many studies have been done to investigate the reaction mechanism in the presence of the Zinc oxide catalysts, from this, two alternatives were proposed, both involving the adsorption of CO and H_2 (Kung, 1980): The mechanism A (Figure 2.1) suggest that the reaction takes place in four consecutive hydrogenation steps.
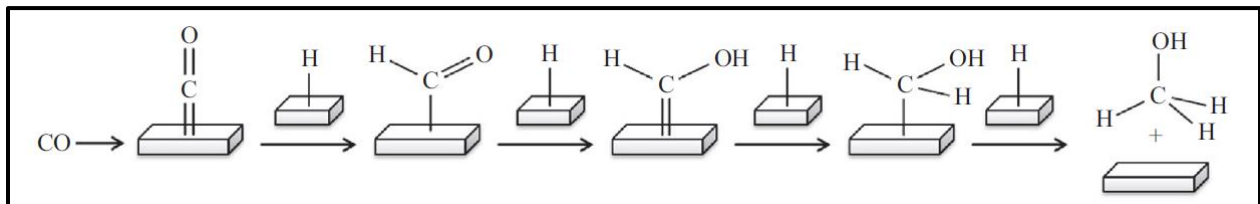
Figure 2.1: Reaction mechanism A (Dalena et al., 2018)

In mechanism B (Figure 2.2) both a CO and a hydroxyl group adsorption on the catalyst surface are involved in the reaction mechanism. The first step takes place by insertion of carbon monoxide to produce a formate intermediate; subsequent by the hydrogenation and dehydration that leads to the formation of methanol, passing through a methoxide intermediate.
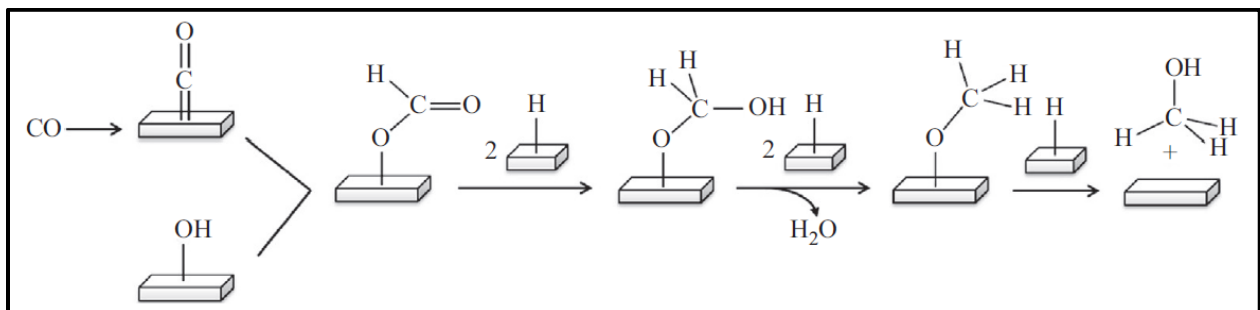
Figure 2.2: Reaction mechanism B (Dalena et al., 2018)

Both mechanisms proposed differ not only for the intermediates formed but also for the way in which they are bonded to the catalyst surface, with a carbon atom in mechanism A and with an oxygen in B. As a consequence, catalytic cycles of ZnO/Cr_2O_3 and ZnO/CuO catalyst were proposed were the active site was assumed to be a cluster of zinc ions with an oxygen vacancy. In agreement with these studies, the interaction between the end oxygen of the adsorbed CO and the cluster electron-deficient vacancy allows the activation of the CO bond (Figure 2.3).
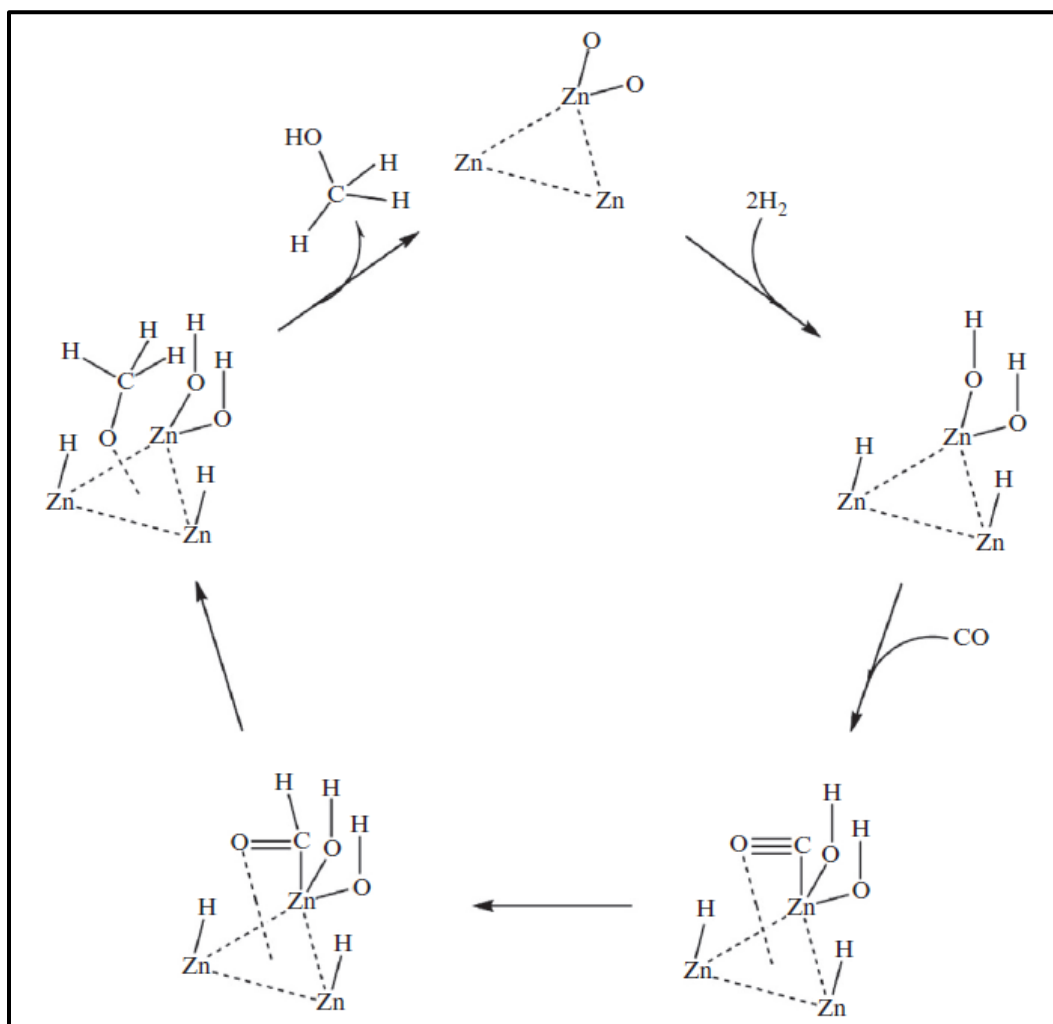
Figure 2.3: Catalytic cycle of ZnO-catalyzed methanol synthesis (Dalena *et al.*, 2018)

2.2.2 The ICI process – low pressure method

The first low-pressure process was developed in 1960 by ICI (now Johnson Matthey). This method presented a new route for methanol synthesis in a pressure range in 35-54 bar and a temperature ranging from 200 to 300 °C. This was possible in part by the uncovering of a new, more active and selective copper-based catalyst ($Cu/ZnO/Al_2O_3$), but also by the development of new advanced purification processes for the synthesis gases, which allowed to use sulfur-chlorine free syngas (van Bennekom *et al.*, 2013; Zhen and Wang, 2015).

Despite the fact that the catalytic power of copper/zinc catalysts in methanol synthesis was already known, this was not exploited commercially before due to their low lifetime and low thermal stability, mostly caused by their deactivation by poisoning and sintering (Chinchen *et al.*, 1988; Sá *et al.*, 2010). These problems were overcome by the addition of alumina, which increases the stability of the Cu/ZnO catalyst and inhibits the thermal formation of Cu crystallites (Peppley *et al.*, 1999; Matsumura and Ishibe, 2009; Sá *et al.*, 2010).

The catalytic phenomena are still under study, most recent research incline into the hypothesis that the oxygen vacancy in the ZnO lattice is responsible for an improvement on the adsorption and transformation of CO and CO_2 while also enhancing the Cu dispersion on the catalyst support (Nakamura, Choi and Fujitani, 2003; Yong *et al.*, 2013; Ganesh, 2014).

Even for all the discrepancies in research, they all agree that the active site for $Cu/Al_2O_3/ZnO$ type of catalysts is the copper, but there are still some disputes about its mechanism. A vast number of investigations are inclined into recognizing the metallic Cu sites as the active catalytic center. Additionally, during the methanol synthesis reaction, oxidized sites of Cu^+ formed from the migration from ZnO to Cu of the ZnO_x species are also recognized to be an active catalytic area. It has been shown that both the Cu^0 and Cu^+ species are important in methanol synthesis, promoting CO_2 and CO hydrogenation respectively; and that the catalytic activity strongly depends on their ratio Cu^+/Cu^0 (Fujitani *et al.*, 1994; Kanai *et al.*, 1994, 1996; Nakamura, Choi and Fujitani, 2003; Ganesh, 2014).

Currently, the accepted microkinetic model shows that methanol can be synthesized by hydrogenation of carbon dioxide through the following intermediates: HCOO, HCOOH, CH_2COOH, CH_2O and CH_3O; and also by hydrogenation of carbon monoxide by HCO, CH_2O, and CH_3O intermediates (Grabow and Mavrikakis, 2011).

The evolution of the processes from BASF high pressure to ICI low pressure led to an increase of 10^5 t/day of methanol production (Mittasch and Pier, 1925; Styhr Petersen, 1972; Kung, 1980; Klier *et al.*, 1982; Pinto, 1983; Wilhelm *et al.*, 2001).
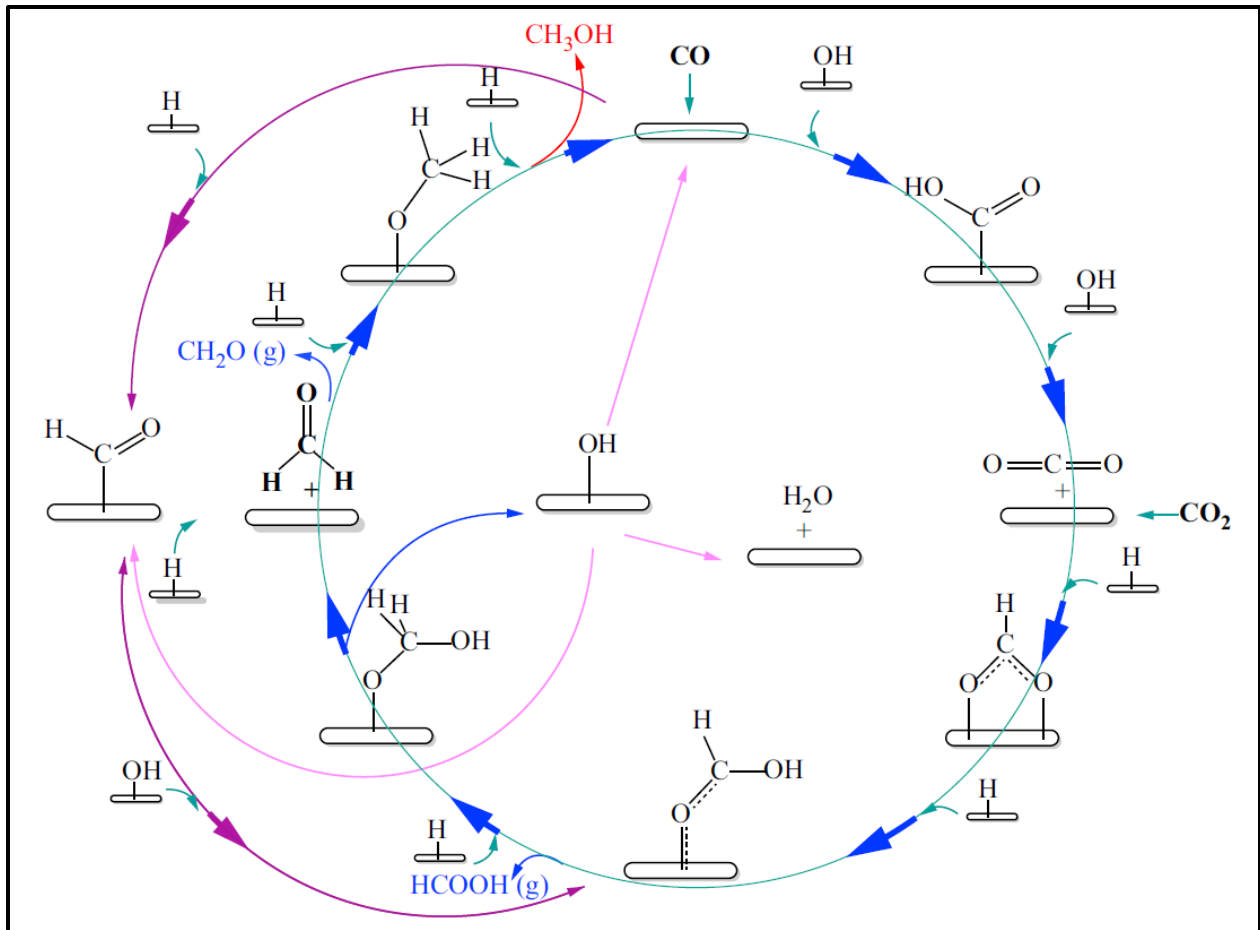
Figure 2.4: Model of mechanism of methanol synthesis on Cu-based catalyst (Dalena *et al.*, 2018)

2.3   Reactors

The synthesis of methanol involves three exothermal reactions; thus, the reactors are designed to provide adapted temperature control. The heat has to be efficiently removed and recovered in order to minimize operative cost, while high conversions per pass are also required in order to minimize separation cost.

Methanol synthesis is performed on mostly two types of reactors, adiabatic reactors and isothermal reactors. Currently, there had been advances on slurry reactors used for liquid phase synthesis of methanol, which allows for a substantial displacement of the reaction's equilibrium on the vapor phase (Lee and Sardesai, 2005; Hu *et al.*, 2008).

The adiabatic reactors design usually settle with one of the three heat control options: (1) Series of fixed bed reactors with quench cooling downstream each reactor, (2) Series of adiabatic fixed bed reactors with the removal of heat via a heat exchange downstream each reactor (Figure 2.5).
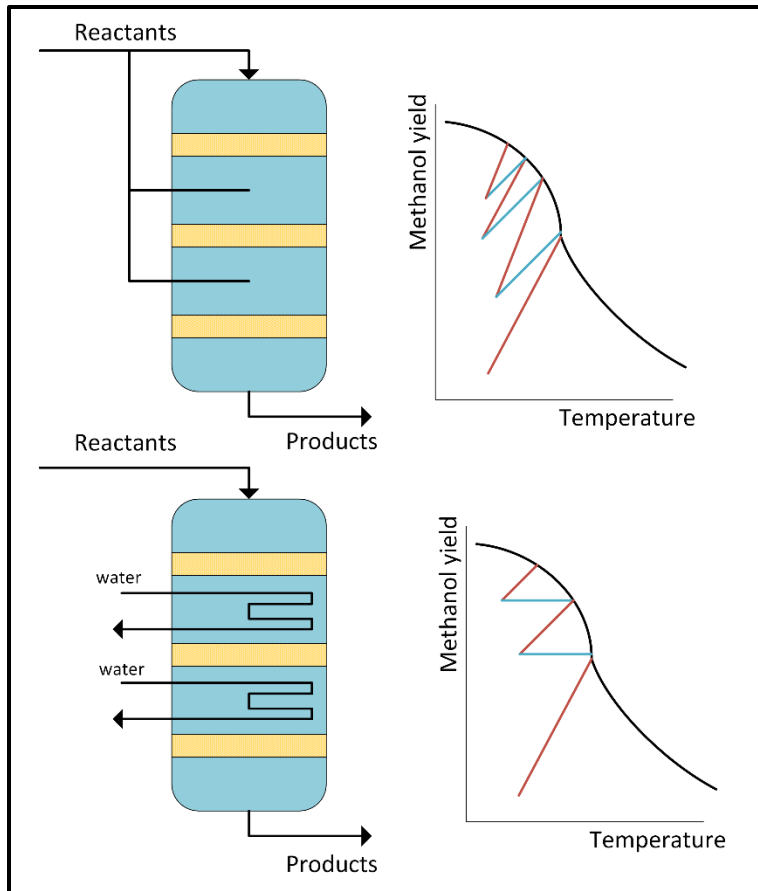
Figure 2.5: left: Adiabatic reactor with direct cooling by quenching; right: Adiabatic reactor with indirect heat exchange

This first alternative is the one adopted by the ICI low pressure process. These types of arrangement are easily configurable, reliable, present a low installation cost and a high production capacity, however, tuning the reactor performance is more complicated and because of the exothermal reactions involved the reagents need a low residential time on each reactor to prevent the over increase in temperature at the end of the pass (which in itself enhance the deactivation of the catalyst by sintering and the byproduct formation), this means the employment of short passes through the reactor which implies low conversion per cycle and, as a result, the need for a high recycle ratio diluting the reagents and increasing cost.

On the other side, isothermal reactors are perpetually cooled with another source (Figure 2.6), this provides better control on the temperature inside the reactor, allowing to maintain the maximum reaction rate as well as optimum temperature profile. As a consequence, it is obtained higher productivity, increased catalyst life, fewer by-products, and a reduction in the recycle ratio if needed.
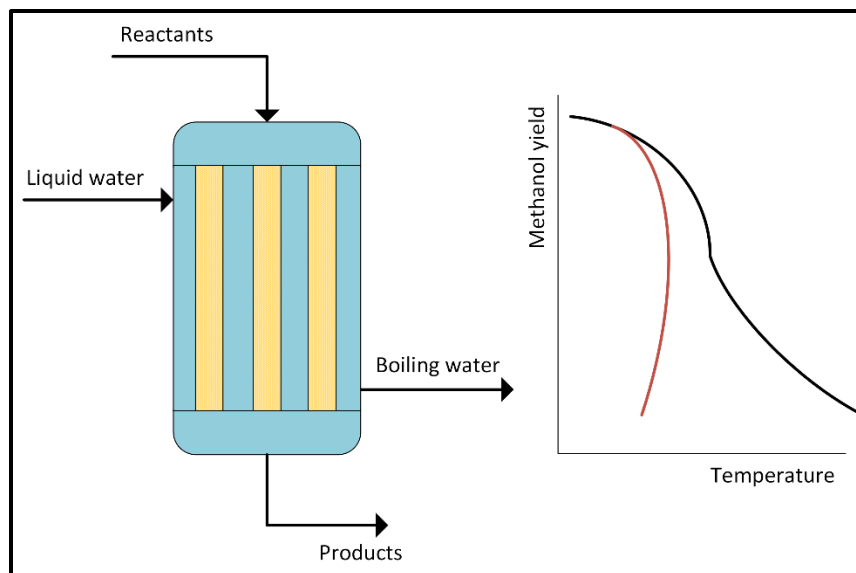
Figure 2.6: Reactor with external cooling

2.4   Catalyst

To abstain from the formation of DME, higher alcohols, and hydrocarbons, methanol synthesis requires a highly selective catalyst that quickly executes the hydrogenation of CO_x to methanol while at the same time does not allow the reaction to advance any further into by-products. The catalytic synthesis of methanol began to be studied before the start of the 19th century, and with it, there have been numerous breakthroughs on the catalyst design and the understanding of the surface mechanism involved.

In 1913 Badische Anilin & Soda Fabrik (BASF) patented a process for the catalytic hydrogenation of carbon monoxide. According to the patent, the synthesis occurred with an excess of CO over hydrogen, 2:1 ratio, at 300-400 °C, 120 atm using the metals cerium, cobalt, molybdenum, or their alkali-containing metallic oxides as catalyst (BASF, 1913).

Then in 1923, Fischer and Tropsch showed that carrying the reaction in a tubular electrically-heated converter at high temperature and pressure, 400-450 °C and 100-150 atm, with a 2:1 ratio of hydrogen over carbon monoxide along with alkali-iron instead of oxide catalysts did not give hydrocarbons but a mixture of oxygen-containing organic compounds such as alcohols, aldehydes, ketones, and fatty acids (Fischer and Hans, 1923).

In 1932, Marek & Hahn declared that the best catalyst consisted of zinc and copper oxide with an admixture of chromium compounds. They also specified that the success of the methanol synthesis depended on the absence of alkali, which would cause subsequently decomposition of the methanol and the production of higher alcohols and oily products, and the complete elimination of all metals except for copper, aluminum and tin from the equipment that come in contact with the reacting gases (Marek and Hahn, 1933).

Catalyst such as metallic iron, nickel, cobalt, platinum and palladium, which promote the decomposition of methanol at low pressures also promote the succeeding reactions:

$$2\,CO \rightleftarrows C + CO$$ <div align="right">*Eq. 2.6*</div>

$$CO + 3\,H_2 \rightleftarrows CH_4 + H_2O$$ <div align="right">*Eq. 2.7*</div>

$$2\,CO + 2\,H_2 \rightleftarrows CH_4 + CO_2$$ <div align="right">*Eq. 2.8*</div>
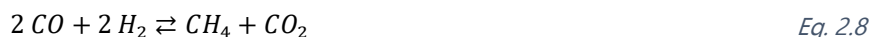
Most of them present a decrease of moles, therefore, forced to the right by pressure. For this reason, such metallic catalysts, despite active in the reduction of carbon monoxide, are pointless for the purpose of producing methanol.

In the following years, a number of processes for the synthesis of methanol based on the use of some particular selective catalysts have been developed in other European countries and in the United States but the results are difficult to grasp in view of the wide differences in the experimental methods being followed. While some studies focused on the catalysis synthesis of methanol, most of the investigations dealt with catalytic decomposition of methanol. The activity of a catalyst was often been measured from the total volume of gas produced while being oblivious of the formation of methyl formate or formaldehyde in addition to that of CO and H_2. In addition, catalysts made with the same precipitation method showed activities which considerably depends on the conditions of the precipitation process (Audibert and Raineau, 1928; Frolich *et al.*, 1929; Natta, 1955).

Natta in 1955 declared that among all the various catalysts which have been proposed for the synthesis of methanol, only those containing ZnO or CuO have a real practical interest. And that the doubtful of the various research results at the time occurred by the fact that the catalytic activity of pure ZnO or CuO is fairly low, while that of mixtures of these compounds with oxides of others metals is much higher (Natta, 1955).

Single oxides catalyst had shown a maximum carbon monoxide conversion of 17.5% (for ZnO). Such single components catalysts are very sensitive to temperature and overheating results in a rapid loss in activity. As zinc oxide is added to chromium catalyst the activity increases until a composition around 60-70% of zinc oxide is reached, after which the activity starts to decrease to a lower value of pure zinc oxide. This same outcome holds for zinc-copper catalyst. Multicomponent catalysts, on the other hand, not only give increase yields of methanol but also resist high temperatures for prolonged periods of time (Marek and Hahn, 1933).

In practice, industrial catalysts have a promoter in the form of a difficult reducible oxide. These promoters have very poor hydrogenation characteristics and high melting points; they also tend to prevent aging due to the growth of crystals of the main catalytic agent.

Zinc oxide has been disclosed as the most selective catalyst for the synthesis of methanol, but his activity, if produced by calcination of precipitation zinc hydroxide, seems to depend on the anion originally combined with the zinc.

Frolich and his team observed that the catalyst obtained by precipitation of $Cu(OH)_2$ with NaOH showed lower activities and selectivity than those precipitated with NH_4OH (Frolich *et al.*, 1929). Hüttig and Goerk tested different catalysts in the decomposition of methyl alcohol observing the best result with catalysts from the decomposition of complex zinc salts (Hüttig and Goerk, 1937). Molstad and Dodge stated that the catalysts precipitated with Na_2CO_3 are more active than those precipitated with ammonia (Ipatiev and Dolgov, 1931; Molstad and Dodge, 1935). A series of tests studying the activity of ZnO obtained from smithsonite presented that the most active catalysts contain, in the form of solid solution, small amounts of other divalent oxides (CdO, MgO, CuO) which are believed to behave as promoters (Kostelitz and Hensinger, 1939). Due to the sensitive structure of the catalyst, even a slight change in the preparation method may cause considerable effects on the catalytic performance and yield (Avgouropoulos and Ioannides, 2003).

A number of authors have detected a relationship between the catalytic activity of ZnO obtained by the thermal decomposition of zinc compounds to the preparation temperature. The size of ZnO crystals increases with an increase in temperature, while the catalytic activity experiences a decrease (Ivannikov, Frost and Shapiro, 1934; Natta and Corradini, 1952). Under similar studies, it has been found that the catalytic activity has a stronger relationship by the crystalline size than by the particle size (Hüttig, Kostelitz and Fehèr, 1931).

On copper oxide containing catalysts, the state at which the copper is present have an influence on the overall catalyst activity, pure copper oxide has a weak catalytic activity (Natta and Corradini, 1952). Reduced copper oxide gives a catalytic activity which depends heavily upon the reduction temperature (Plotnikov and Ivanov, 1934; Veltistova, Dolgov and Karpov, 1934).

A more recent investigation was carried out with the purpose to define what causes the high activity of binary Copper-Zinc Oxide catalysts systems compared to their individual components. The most active catalyst was characterized by having a large amount of amorphous copper (Bulko *et al.*, 1979). BET surface tests have shown no dramatic increase in samples with a large amount of amorphous copper, contrary to what was expected if amorphous copper were dispersed as very small particles (Herman *et al.*, 1979). Significant amounts of copper were found in the zinc oxide phase of the catalyst showing that most if not all amorphous copper is located in the zinc oxide crystallites (Mehta *et al.*, 1979). Further experiments showed that the copper was not accumulated on the zinc oxide crystallite surface (Klier, 1982).

The copper solution in the zinc oxide characterized by the analytical and physical methods was found to exist only after a mild reduction of the calcined catalysts. Before reduction, the solubility of CuO in ZnO is limited to 4-6% (Chapple and Stone, 1964; Schiavello, Pepe and De Rossi, 1974) and after more severe reduction, the optical spectra begin to resemble a superposition of those of pure copper metal and zinc oxide. For this reason, the dispersed copper species were assigned the valences state +1, more like electron-deficient copper atoms with strong electronic overlap with the host zinc oxide lattice than as isolated Cu^+ ions (Bulko *et al.*, 1979).

The methanol synthesis mechanism – more deeply discussed in section 2.5 - is thought to follow an approximation of the scheme depicted in Figure 2.7. As a consequence of this mechanism, the copper surface is covered with formate ($CHOO^-$), formyl ($-CHO$), methoxy species ($-OCH_3$) and oxygen to an extent determined by the kinetics and relative rates of the various reaction steps (Chinchen, Waugh and Whan, 1986).
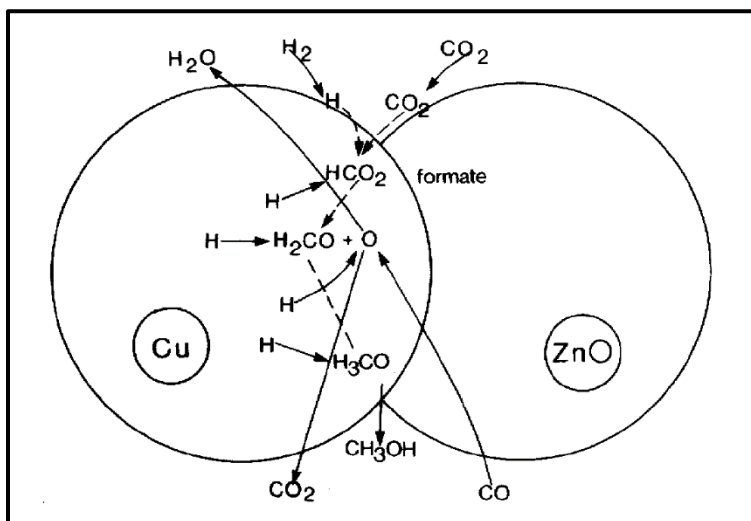
Figure 2.7: Mechanism of methanol synthesis on a Cu/ZnO/Al2O3 catalysts from a CO, CO2, H2 feed (Chinchen, Waugh and Whan, 1986)

A more recent study over a Cu/Zn/Al/Zr catalyst reported similar mechanics where Cu absorbed CO_2 and Zn absorbed H_2 forming the same intermediates (An *et al.*, 2007).

The adsorption of methanol on oxidized and reduced copper on silica catalysts has been studied using in situ FTIR spectroscopy (Peppley *et al.*, 1999). This procedure was able to show that methanol readily absorbs dissociatively on copper to form adsorbed methoxy species at temperatures as low as 295 K. At higher temperatures, the methoxy groups dehydrogenate to form formaldehyde, or its isomer oxymethylene, which subsequently is converted to a formate (Wachs and Madix, 1978; Millar, Rochester and Waugh, 1991). These observations have been confirmed with the diffuse reflectance in situ Fourier transform infrared spectroscopy (DRIFTS) (Millar, Rochester and Waugh, 1991).

More recent research over CZA catalysts have shown that Zn-Cu undergoes surface oxidation under the reaction conditions so that surface Zn transforms into ZnO and allows Zn-Cu to reach the activity of ZnO/Cu with the same Zn coverage and highlight a synergy of Cu and ZnO at the interface facilitating methanol synthesis via formate intermediates (Kattel *et al.*, 2017).

Another study observed a boost on methanol synthesis over copper and zinc oxide nanoparticles and the relation of this promotion by Zn atoms migrating in the Cu surface as a function of the size-dependent thermodynamics activities of the Cu and ZnO nanoparticles (Kuld *et al.*, 2016).

Overall, a synergetic effect between Cu and ZnO exist as a result of three different phenomena (Angelo *et al.*, 2015): changing of Cu particles morphology by a wetting/non-wetting effect of the Cu/ZnO system, migration of ZnO_x species on the surface of Cu particles because of the formation of a Cu-Zn surface alloy, which enhance copper activity; and hydrogen dissociation on ZnO, which is a source of H_2 storage (Grabow and Mavrikakis, 2011).

2.5 Kinetic models and mechanism

Although low-pressure methanol synthesis is an important industrial process, the kinetics studies on this subject have just recently reached an agreement, especially on the role of CO_2, most of the models published in the past described methanol formation from CO only. The only role of CO_2 in these models, if present, is restricted to competitive adsorption on the active sites of the catalyst.

Early kinetic models were delivered for the ZnO/Cr_2O_3 catalyst of the high-pressure process (BASF process), which has now almost completely been abandoned in favor of the low-pressure technology. One of the first of this kind was the model proposed by Natta (Natta, 1955). Natta assumed that only the hydrogenation of CO occurs (Eq. 2.1), in which he proposed the trimolecular reaction of CO and molecular hydrogen to be rate determining.

$$ r = \frac{f_{CO}f_{H_2} - \dfrac{f_{CH_3OH}}{K_{eq}}}{\left(A + Bf_{CO} + Cf_{H_2} + Df_{CH_3OH}\right)^3} \qquad \textit{Eq. 2.9} $$

Bakemeier (Bakemeier, Laurer and Schroeder, 1970) noted an important discrepancy between their experimental and Natta's predictions, particularly in the case of CO_2 rich feeds. For this reason, a CO_2 dependency was introduced in the equation in the shape of a Langmuir type isotherm by assuming the methanol desorption to be rate determinizing, the authors ended up with:

$$ r_{CH_3OH} = \frac{Ae^{-E/RT}\left[p_{CO}^m p_{H_2}^n \left(1 - \left(p_{CH_3OH}/p_{CO}p_{H_2}^2 K_2^*\right)\right)\right]}{1 + De^{-E/RT}\, p_{CO_2}/p_{H_2}} \qquad \textit{Eq. 2.10} $$

Leonov (Leonov *et al.*, 1973) was the first model methanol synthesis kinetics over a $Cu/ZnO/Al_2O_3$ catalyst. Their model again assumed CO to be the source of carbon in methanol and did not account for the influence of CO_2 in the feed.

$$ r_{CH_3OH} = k\left(\frac{p_{CO}^{0.5}p_{H_2}}{p_{CH_3OH}^{0.66}} - \frac{p_{CH_3OH}^{0.34}}{p_{CO}^{0.5}p_{H_2}K_2^*}\right) \qquad \textit{Eq. 2.11} $$

Whereas these first authors used a more or less correlative approach, a number of later contributions focused on effectively implementing detailed mechanistic considerations in the kinetic model. Klier (Klier *et al.*, 1982) no longer considered CO to be the only source of carbon in methanol, but still the most important. His experimental variation of the p_{CO}/p_{CO_2} ratio, at fixed total pressure and hydrogen concentration revealed a maximum in the synthesis rate. They hold

strong CO_2 adsorption on catalysts surface responsible for reaction rate decrease at low p_{CO}/p_{CO_2}, while at high ratios an excessive reduction of the catalyst was thought to take place. The ratio of the number of active oxidized sites and the inactive reduced sites is solely determined by the p_{CO}/p_{CO_2} through a redox-like mechanism. They further assumed competitive adsorption of CO_2 and CO or H_2 and accounted for the direct hydrogenation of CO_2 by an empirical term. This led to the following equation:

$$r_{CH_3OH} = k_{r_{CH_3OH}} \left(1 + \frac{p_{CO}}{k_{redox}^{eq}p_{CO_2}}\right)^{-3} \frac{K_{CO}K_{H_2}^2 \left(p_{CO}p_{H_2}^2 - p_{CH_3OH}/K_{r_{CH_3OH}}^{eq}\right)}{\left(1 + K_{CO}p_{CO} + K_{CO_2}p_{CO_2} + K_{H_2}p_{H_2}\right)}$$

<div align="right">Eq. 2.12</div>

These equations later served as a base for the work of McNeil and his team (Schack, McNeil and Rinker, 1989), who expanded on the mechanism of the direct hydrogenation of CO_2 and the possible role of ZnO as a hydrogen reservoir. Despite the much larger number of parameters in the resulting model, the latter authors did not manage to show a significantly better agreement between the experimental and the simulated results that the already obtained by Klier (Klier *et al.*, 1982).

Villa and his team realized that a thorough modeling of the methanol synthesis system should also involve a description of the water gas shift reaction. Assuming thereby again that the hydrogenation of CO is the only route to methanol, this resulted in the following set of equations implying that the generation of methanol and the water gas shift reaction occur on different types of sites (Villa *et al.*, 1985).

$$r_{CH_3OH} = \frac{f_{CO}f_{H_2}^2 - f_{CH_3OH}/K_2^*}{\left(A + Bf_{CO} + Cf_{H_2} + Gf_{CO_2}\right)^3}$$

<div align="right">Eq. 2.13</div>

$$r_{RWGS} = \frac{f_{CO_2}f_{H_2} - f_{CO}f_{H_2O}K_3^*}{M^2}$$

<div align="right">Eq. 2.14</div>

Graff (Graaf, Stamhuis and Beenackers, 1988) considered both the hydrogenation of CO and CO_2 as well as the water gas shift reaction. Inspired by the work of Herman (Herman *et al.*, 1979), the authors proposed a dual site mechanism, adsorbing CO and CO_2 on an s_1 type site and H_2 and water on as site s_2. The formation of methanol from CO and CO_2 occurs through successive hydrogenation, while the water gas shift reaction proceeds along a formate route. Assuming the ad- and desorptions to be in equilibrium and taking every elementary step in each of the three overall reactions in its turn as rate determining, the authors ended up with 48 possible models. Statistical discrimination allowed them to select the following final set of equations were the step A3, B2 and C3 surfaced as the rate determining (Table 2.1).

$$r_{CO\rightarrow CH_3OH} = \frac{k_1 K_{CO}\left(f_{CO}f_{H_2}^{1.5} - \frac{f_{CH_3OH}}{f_{H_2}^{0.5}K_1^{eq}}\right)}{1 + K_{CO}f_{CO} + K_{CO_2}f_{CO_2}\left(f_{H_2}^{0.5} + \left(K_{H_2O}/k_{H_2}^{0.5}\right)f_{H_2O}\right)}$$

<div align="right">Eq. 2.15</div>

$$r_{RWGS} = \frac{k_2 K_{CO_2}\left(f_{CO_2} f_{H_2} - \dfrac{f_{H_2O} f_{CO}}{K_2^{eq}}\right)}{1 + K_{CO} f_{CO} + K_{CO_2} f_{CO_2}\left(f_{H_2}^{0.5} + \left(K_{H_2O} \big/ k_{H_2}^{0.5}\right) f_{H_2O}\right)} \qquad \text{Eq. 2.16}$$

$$r_{CO_2 \rightarrow CH_3OH} = \frac{k_3 K_{CO_2}\left(f_{CO_2} f_{H_2}^{1.5} - \dfrac{f_{CH_3OH} f_{H_2O}}{f_{H_2}^{1.5} K_3^{eq}}\right)}{1 + K_{CO} f_{CO} + K_{CO_2} f_{CO_2}\left(f_{H_2}^{0.5} + \left(K_{H_2O} \big/ k_{H_2}^{0.5}\right) f_{H_2O}\right)} \qquad \text{Eq. 2.17}$$

In doing this, however, the authors failed to account for the fact that some intermediates feature in two different overall reactions. This implies that the model simultaneously predicts two different concentrations of one and the same intermediate like formyl and methoxy species.

Surface phenomena	Elementary step	Driving-force
Adsorption	$CO + s_1 \rightleftarrows CO(s_1)$	
	$CO_2 + s_1 \rightleftarrows CO_2(s_1)$	
	$H_2 + 2(s_2) \rightleftarrows 2H(s_2)$	
	$H_2O + s_2 \rightleftarrows H_2O(s_2)$	
CO hydrogenation	$(A_1): CO(s_1) + H(s_2) \rightleftarrows HCO(s_1) + s_2$	$f_{CO} f_{H_2}^{0.5} - f_{CH_3OH}/\left(f_{H_2}^{1.5} K_{p_1}^o\right)$
	$(A_2): HCO(s_1) + H(s_2) \rightleftarrows H_2CO(s_1) + s_2$	$f_{CO} f_{H_2} - f_{CH_3OH}/\left(f_{H_2} K_{p_1}^o\right)$
	$(A_3): H_2CO(s_1) + H(s_2) \rightleftarrows H_3CO(s_1) + s_2$	$f_{CO} f_{H_2}^{1.5} - f_{CH_3OH}/\left(f_{H_2}^{0.5} K_{p_1}^o\right)$
	$(A_4): H_3CO(s_1) + H(s_2) \rightleftarrows CH_3OH + s_1 + s_2$	$f_{CO} f_{H_2}^2 - f_{CH_3OH}/K_{p_1}^o$
Water-gas shift	$(B_1): CO_2(s_1) + H(s_2) \rightleftarrows HCO_2(s_1) + s_2$	$f_{CO_2} f_{H_2}^{0.5} - f_{CO} f_{H_2O}/\left(f_{H_2}^{0.5} K_{p_2}^o\right)$
	$(B_2): HCO_2(s_1) + H(s_2) \rightleftarrows CO(s_1) + H_2O(s_2)$	$f_{CO_2} f_{H_2} - f_{CO} f_{H_2O}/K_{p_2}^o$
CO$_2$ hydrogenation	$(C_1): CO_2(s_1) + H(s_2) \rightleftarrows HCO_2(s_1) + s_2$	$f_{CO_2} f_{H_2}^{0.5} - f_{CH_3OH} f_{H_2O}/\left(f_{H_2}^{2.5} K_{p_3}^o\right)$
	$(C_2): HCO_2(s_1) + H(s_2) \rightleftarrows H_2CO_2(s_1) + s_2$	$f_{CO_2} f_{H_2} - f_{CH_3OH} f_{H_2O}/\left(f_{H_2}^2 K_{p_3}^o\right)$
	$(C_3): H_2CO_2(s_1) + H(s_2) \rightleftarrows H_3CO_2(s_1) + s_2$	$f_{CO_2} f_{H_2}^{1.5} - f_{CH_3OH} f_{H_2O}/\left(f_{H_2}^{1.5} K_{p_3}^o\right)$
	$(C_4): H_3CO_2(s_1) + H(s_2) \rightleftarrows H_2CO(s_1) + H_2O(s_2)$	$f_{CO_2} f_{H_2}^2 - f_{CH_3OH} f_{H_2O}/\left(f_{H_2} K_{p_3}^o\right)$
	$(C_5): H_2CO(s_1) + H(s_2) \rightleftarrows H_3CO(s_1) + s_2$	$f_{CO_2} f_{H_2}^{2.5}/f_{H_2O} - f_{CH_3OH}/\left(f_{H_2}^{0.5} K_{p_3}^o\right)$
	$(C_6): H_3CO(s_1) + H(s_2) \rightleftarrows CH_3OH + s_1 + s_2$	$f_{CO_2} f_{H_2}^3/f_{H_2O} - f_{CH_3OH}/K_{p_3}^o$

Table 2.1: Graaf reaction scheme for both hydrogenation reactions and the water gas shift reaction (Graaf, Stamhuis and Beenackers, 1988)

Parallel to this, a Russian research group led by Rozovskii developed a number of kinetic models for the Cu/ZnO/Al$_2$O$_3$ catalyst. Since neither of these groups ever succeeded in producing methanol from a dry mixture of CO and hydrogen, the models are all based on the direct hydrogenation of CO$_2$ to methanol, while the majority also accounts for the occurrence of the

water gas shift reaction. Malinovskaya (Malinovskaya *et al.*, 1987) compared a number of these models using own experimental data and selected the following set of equations, originally presented by Mochalin (Mochalin, Lin and Rozovskii, 1984).

$$r_{CH_3OH} = \frac{f_{CO}f_{H_2}^2 - \left.f_{CH_3OH}\right/K_2^*}{\left(A + Bf_{CO} + Cf_{H_2} + Gf_{CO_2}\right)^3} \qquad \text{Eq. 2.18}$$

$$r_{RWGS} = \frac{f_{CO_2}f_{H_2} - f_{CO}f_{H_2O}K_3^*}{M^2} \qquad \text{Eq. 2.19}$$

Unfortunately, the authors did not expand on the physical background of the model, nor did they mention the numerical value of the different parameters in the model.

Two years after, Vanden (Vanden Bussche and Froment, 1996), based on the results of Chinchen (Chinchen *et al.*, 1988) and Rozovskii (Rozovskii, 1989) assumed that CO_2 is the main source of carbon in methanol by hydrogenation and also accounting for the water gas shift redox mechanism.

They assumed both reactions proceed on the copper phase of the catalyst, where the role of ZnO is limited to structural promotion. A mechanism proposed, occurring exclusively and completely on the copper phase, is presented in Table 2.2.

Elementary step		
$H_2 + 2s \rightleftarrows 2H(s)$	K_{112}	
$CO_2 + s \rightleftarrows O(s) + CO$	(k_1, K_1)	(rds)
$CO_2 + O(s) + s \rightleftarrows CO_3(2s)$	(K_2)	
$CO_3(2s) + H(s) \rightleftarrows HCO_3(2s) + s$	(K_3)	
$HCO_3(2s) + s \rightleftarrows HCO_2(2s) + O(s)$	(K_4)	
$HCO_2(2s) + H(s) \rightleftarrows H_2CO_2(2s) + s$	(k_{5a})	(rds)
$H_2CO_2(2s) \rightleftarrows H_2CO(s) + O(s)$	(K_{5b})	
$H_2CO(s) + H(s) \rightleftarrows H_3CO(s) + s$	(K_6)	
$H_3CO(s) + H(s) \rightleftarrows CH_3OH + 2s$	(K_7)	
$O(s) + H(s) \rightleftarrows OH(s) + s$	(K_8)	
$OH(s) + H(s) \rightleftarrows H_2O(s) + s$	(K_9)	
$H_2O(s) \rightleftarrows H_2O + s$	(K_{H_2O})	

Table 2.2: Reaction scheme for the synthesis of methanol and the water gas shift reaction (Vanden Bussche and Froment, 1996)

Both H_2 and CO_2 absorb dissociative on the copper surface. The oxidizing adsorption of CO_2 on metallic copper is promoted by traces of surface oxygen or alkaline species. On the oxidized copper surface, carbonate structures are formed by further adsorption of CO_2. These carbonates are quickly hydrogenated, first to bicarbonate structures and subsequently to Cu formate, formaldehyde, methoxy species, and finally methanol. In this sequence, the rate determining step is the hydrogenation of the formate, which is generally accepted to be the longest living intermediate in methanol synthesis on copper (Bowker *et al.*, 1988; Rozovskii, 1989; Neophytides, Marchi and Froment, 1992). At the second stage in the hydrogenation of CO_2 to methanol, surface oxygen is released from the molecule, this specie is also hydrogenated by the available hydrogen atoms, yielding hydroxyl groups and subsequently water, which is known to desorb relatively slowly. In this sequence of reactions, the dissociative adsorption of CO_2 is the rate determining step (Nakamura, Campbell and Campbell, 1990; Ernst *et al.*, 1991; Fujita *et al.*, 1992). The final expression presented by Vanden is the following:

$$r_{CO_2 \to CH_3OH} = \frac{k'_{5a} K'_2 K_3 K_4 K_{H_2} p_{CO_2} p_{H_2} \left[1 - \left(\frac{1}{K^*} \right) \left(\frac{p_{H_2O} \cdot p_{CH_3OH}}{p_{CO_2} \cdot p_{H_2}^3} \right) \right]}{\left(1 + \left(\frac{K_{H_2O}}{K_8 K_9 K_{H_2}} \right) \left(\frac{p_{H_2O}}{p_{H_2}} \right) + \sqrt{K_{H_2} p_{H_2}} + K_{H_2O} p_{H_2O} \right)^3}$$

Eq. 2.20

$$r_{RWGS} = \frac{k'_1 p_{CO_2} \left[1 - K_3^* \left(\frac{p_{H_2O} p_{CO}}{p_{CO_2} p_{H_2}} \right) \right]}{1 + \left(\frac{K_{H_2O}}{K_8 K_9 K_{H_2}} \right) \left(\frac{p_{H_2O}}{p_{H_2}} \right) + \sqrt{K_{H_2} p_{H_2}} + K_{H_2O} p_{H_2O}}$$

Eq. 2.21

Despite many useful kinetics models for methanol synthesis, very few investigations have addressed the development of kinetic models based on three-site adsorption ($Cu^{1+}, Cu^0, and\ ZnO$). Park and his team modified detailed elementary steps for both CO and CO_2 hydrogenation based on two-site adsorption by considering an additional adsorption site for CO_2 to develop a model for the three-site adsorption (Park, Park, *et al.*, 2014). They observed different rate determining step: the surface reaction of a methoxy species, the hydrogenation of the formate intermediate HCO_2, and the formation of a formate intermediate for CO and CO_2 hydrogenations and water gas shift reactions. Table 2.3 displays the elementary reactions for CO and CO_2 hydrogenation and the water gas shift reaction.

Surface phenomena	Elementary step	Equilibrium constant
Adsorption	$CO + s_1 \rightleftarrows CO(s_1)$	$K_{CO} = \dfrac{\theta_{CO(s_1)}}{f_{CO}\theta_{s_1}}$
	$CO_2 + s_3 \rightleftarrows CO_2(s_3)$	$K_{CO_2} = \dfrac{\theta_{CO_2(s_3)}}{f_{CO_2}\theta_{s_3}}$
	$H_2 + 2(s_2) \rightleftarrows 2H(s_2)$	$K_{H_2} = \dfrac{\theta^2_{H(s_2)}}{f_{H_2}\theta^2_{s_2}}$
	$H_2O + s_2 \rightleftarrows H_2O(s_2)$	$K_{H_2O} = \dfrac{\theta_{H_2O(s_2)}}{f_{H_2O}\theta_{s_2}}$
CO hydrogenation	$(A_1): CO(s_1) + H(s_2) \rightleftarrows HCO(s_1) + s_2$	K_{A_1}
	$(A_2): HCO(s_1) + H(s_2) \rightleftarrows H_2CO(s_1) + s_2$	K_{A_2}
	$(A_3): H_2CO(s_1) + H(s_2) \rightleftarrows H_3CO(s_1) + s_2$	K_{A_3}
	$(A_4): H_3CO(s_1) + H(s_2) \rightleftarrows CH_3OH + s_1 + s_2$	K_{A_4}
Water-gas shift	$(B_1): CO_2(s_3) + H(s_2) \rightleftarrows HCO_2(s_3) + s_2$	K_{B_1}
	$(B_2): HCO_2(s_3) + H(s_2) \rightleftarrows CO(s_3) + H_2O(s_2)$	K_{B_2}
CO₂ hydrogenation	$(C_1): CO_2(s_3) + H(s_2) \rightleftarrows HCO_2(s_3) + s_2$	K_{C_1}
	$(C_2): HCO_2(s_3) + H(s_2) \rightleftarrows H_2CO_2(s_3) + s_2$	K_{C_2}
	$(C_3): H_2CO_2(s_3) + H(s_2) \rightleftarrows H_3CO_2(s_3) + s_2$	K_{C_3}
	$(C_4): H_3CO_2(s_3) + H(s_2) \rightleftarrows H_2CO(s_3) + H_2O(s_2)$	K_{C_4}
	$(C_5): H_2CO(s_3) + H(s_2) \rightleftarrows H_3CO(s_3) + s_2$	K_{C_5}
	$(C_6): H_3CO(s_3) + H(s_2) \rightleftarrows CH_3OH + s_3 + s_2$	K_{C_6}

Table 2.3: Park elementary reactions for the synthesis of methanol (Park, Park, *et al.*, 2014)

It is worth noticing that Park model included the dehydration of methanol to dimethyl ether since experimental data showed the production of it, while other byproducts such as higher alcohol, methane, and hydrocarbons were detected with trace (negligible) amount.

The final model presented by Park's team considered the steps (A_3), (B_2), and (C_3) from Table 2.3 to be the rate determining steps for CO hydrogenation, WGS reaction, and CO$_2$ hydrogenation respectively. All other steps were assumed to be at equilibrium. From this, they formulate the following reaction rates expressions:

$$r_{CO \rightarrow CH_3OH} = \frac{k'_{r_{CO \rightarrow CH_3OH}}K_{CO}\left[f_{CO}f_{H_2}^{0.5} - f_{CH_3OH}/\left(f_{H_2}^{0.5} \cdot K_{r_{CO \rightarrow CH_3OH}}\right)\right]}{(1 + K_{CO}f_{CO})\left(1 + K_{H_2}^{0.5}f_{H_2}^{0.5} + K_{H_2O}f_{H_2O}\right)}$$ *Eq. 2.22*

$$r_{RWGS} = -\frac{k'_{r_{RWGS}}K_{CO_2}\left[f_{CO_2}f_{H_2} - f_{CO}f_{H_2O}/K_{r_{RWGS}}\right]}{(1 + K_{CO}f_{CO_2})\left(1 + K_{H_2}^{0.5}f_{H_2}^{0.5} + K_{H_2O}f_{H_2O}\right)}$$ *Eq. 2.23*

$$r_{CO_2 \rightarrow CH_3OH} = \frac{k'_{r_{CO_2 \rightarrow CH_3OH}}K_{CO_2}\left[f_{CO_2}f_{H_2}^{0.5} - f_{H_2O}f_{CH_3OH}/\left(f_{H_2}^{1.5}K_{r_{CO_2 \rightarrow CH_3OH}}\right)\right]}{(1 + K_{CO_2}f_{CO_2})\left(1 + K_{H_2}^{0.5}f_{H_2}^{0.5} + K_{H_2O}f_{H_2O}\right)}$$ *Eq. 2.24*

For the dimethyl ether production, Park's model employed the reaction rate equation published by Ng and his team (Ng, Chadwick and Toseland, 1999).

$$r_{DME} = \frac{k_{DME} K_{CH_3OH}^2 \left[C_{CH_3OH}^2 - \left(C_{H_2O} C_{DME} \right) / K_{P,DME} \right]}{\left(1 + 2\sqrt{K_{CH_3OH} C_{CH_3OH}} + K_{H_2O,DME} C_{H_2O} \right)^4}$$

<div align="right">Eq. 2.25</div>

Chapter 3:

Study of the kinetics model for the synthesis of methanol from syngas on Cu/ZnO/Al$_2$O$_3$ catalysts

Kinetic data plays an important role in designing a chemical reactor and, as a consequence, the whole plant. Lamentably, there isn't an agreement in the literature on a single kinetics model for methanol synthesis from syngas, not even for the same types of catalysts. The objective of this chapter is to use experimental data to test literature's most accepted kinetic models and apply to them a reparametrization process by a minimum mean square error approach.

The experimental data was completely acquired by the Chemistry department at Milano University. They tested two types of Cu/ZnO/Al$_2$O$_3$ (CZA) catalysts, a commercial and a laboratory synthetize one, over two set of temperatures, 240°C and 260°C, at 20 bars for a different set of feed compositions.

3.1   Experiment description

Figure 3.1 represents a schematic view of the bench scale setup that was used for the acquisition of the kinetic data. In the feed section, N$_2$ and the reactants: CO, CO$_2$, and H$_2$ were led through a set of flow controllers that inserted the corresponded flow into a gas mixer to subsequently enter the reactor. A pressure controller back-regulates the pressure inside the reactor. An electrical furnace heats the reactor to the desired temperature. The reagents flow from the top to the bottom of the reactor, in a fixed bed configuration. After the reactor, a cold trap (T = -8 °C) capture the condensates (methanol and water). A micro gas chromatography device (Agilent 3000A) equipped with a plotQ and a Molsieve columns samples the existing gases every 1 hour and calculates the flow of CO and CO$_2$ exiting the reactor. This device also detects the methanol that is not condensed as well.

A totalizer (Ritter brand) measures the total volume of gases exiting the reactor. A gas chromatography device (Fision 8000) and a Total Organic Carbon analysis device (Shimadzu brand) determined the concentration of methanol in the cold trap at the end of the test.

The reactor (Figure 3.2) consisted of a copper tubular tube with an internal diameter of ¼ of an inch, 1 mm of thickness and a length of 56 cm. This reactor was able to work at a maximum temperature of 400°C and a pressure of 100 bar.

Prior to the test, 10 $\left[\frac{NmL}{min}\right]$ of H$_2$ reduced the catalyst *in situ* at 300 $[°C]$ for 3 hours.

Table 3.1 presents the characterization of both types of catalysts used in the study. The synthesized catalyst was prepared following the precipitation method.
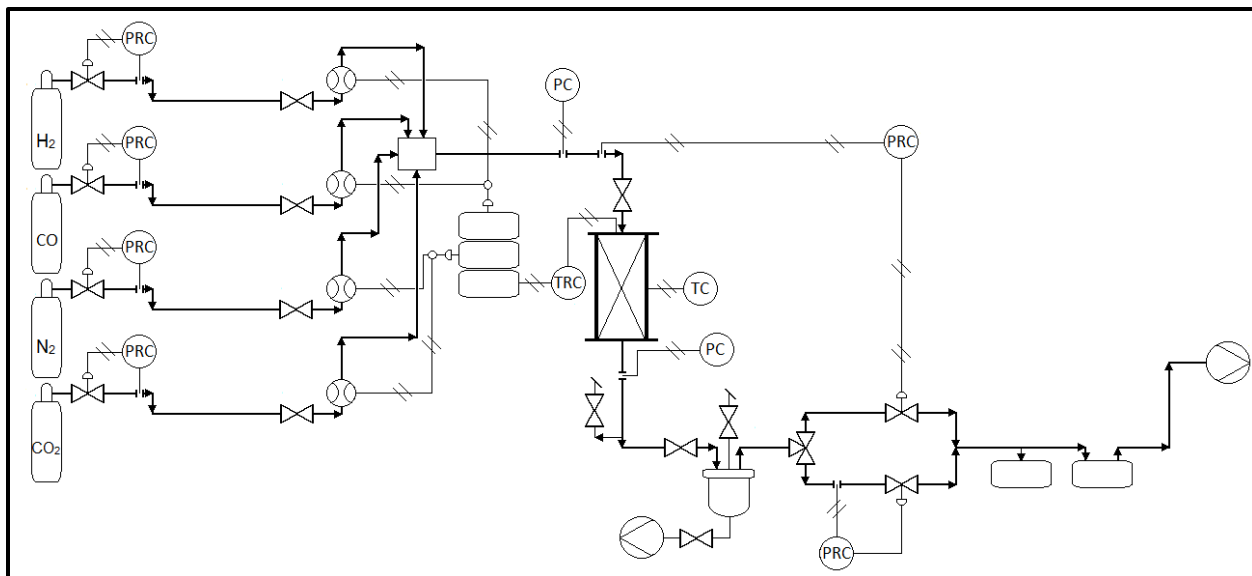
Figure 3.1: Bench-Scale Plant

Figure 3.2: Experimental reactor (disjointed)

Composition	CZA commercial		CZA synthesize		
	CuO 63.5%	ZnO 24.7%	CuO 60%	ZnO 30%	Al$_2$O$_3$ 10%
	Al$_2$O$_3$ 10%	MgO 1.3%			
BET surface area [m^2/g]	100.18 ± 1.1		94.93 ± 0.42		
Langmuir surface area [m^2/g]	120.49		120.90		
BHJ pore volume [cm^3/g]	0.1861		0.4942		
Mean pore size [nm]	6.8		18.19		

Table 3.1: Catalysts characterization

3.2 Kinetic models selected

There is a vast number of kinetic models for the methanol synthesis on the literature, they differ from each other on the type of assumptions applied, operative conditions used, parametrization approach, and the type of catalyst and reactor for which they are valid. On Table 3.2 there is a chronological presentation of the most important models and their operative conditions and catalyst used.

For this work, three different models were selected to be studied:

1. Vanden Bussche & Froment model (Vanden Bussche and Froment, 1996)
2. Graaf's model (Graaf, Stamhuis and Beenackers, 1988)
3. Park's model (Park, Park, *et al.*, 2014)

They were chosen by being all formulated under operating conditions and catalyst of interest. Vanden and Graaf models have been used on numerous scientific reports, while Park model is one of the most current models regarding the methanol synthesis formulated on the basis of a three-site adsorption mechanism (Table 2.3). Since there wasn't any report on a considerable amount of DME found at the cold trap, the reaction rate for DME production was withdrawn from Park's model.

The molar fraction fugacities of each component are calculated by the Soave-Redlich-Kwong equation of state (Soave, 1972).

Author	Reaction rates expression	Operating conditions
Natta (1955)	$$r = \frac{f_{CO}f_{H_2} - \frac{f_{CH_3OH}}{K_{eq}}}{\left(A + Bf_{CO} + Cf_{H_2} + Df_{CH_3OH}\right)^3}$$	cat: $Cu\|ZnO\|Cr_2O_3$ $T \in 573 - 603\ [K]$ $P \in 202 - 319\ [bar]$
Leonov et al. (1973)	$$r_{CO\rightarrow CH_3OH} = k\left(\frac{p_{CO}^{0.5}p_{H_2}}{p_{CH_3OH}^{0.66}} - \frac{p_{CH_3OH}^{0.34}}{p_{CO}^{0.5}p_{H_2}K_2^*}\right)$$	cat: $Cu\|ZnO\|Cr_2O_3$ $T \in 493 - 533\ [K]$ $P \in 4 - 5.5\ [MPa]$
Schermuly and Luft (1977)	$$r_{CO\rightarrow CH_3OH} = \frac{k\left(f_{CO}f_{H_2}^2 - f_{CH_3OH}/K_{eq}\right)}{\left(1 + Af_{CO} + Bf_{H_2} + Cf_{CH_3OH} + Df_{CO_2}\right)^2}$$	cat: CuO- containing $T \in 498 - 523\ [K]$ $P = 75\ [bar]$
Klier et al (1982)	$$r_{CO\rightarrow CH_3OH} = k_{r_{CO\rightarrow CH_3OH}}\left(1 + \frac{p_{CO}}{k_{redox}^{eq}p_{CO_2}}\right)^{-3}\frac{K_{CO}K_{H_2}^2\left(p_{CO}p_{H_2}^2 - p_{CH_3OH}/K_{r_{CO\rightarrow CH_3OH}}^{eq}\right)}{\left(1 + K_{CO}p_{CO} + K_{CO_2}p_{CO_2} + K_{H_2}p_{H_2}\right)}$$ $$r_{CO_2\rightarrow CH_3OH} = k_{r_{CO_2\rightarrow CH_3OH}}\left(p_{CO_2} - \frac{p_{CH_3OH}p_{H_2O}}{K_{r_{CO_2\rightarrow CH_3OH}}^{eq}p_{H_2}^3}\right)$$	cat: $CuO\|ZnO$ $T \in 498 - 523\ [K]$ $P = 7.5\ [MPa]$
Seyfert and Luft (1985)	$$r_{CO\rightarrow CH_3OH} = \frac{k\left(f_{CO}f_{H_2}^2 - f_{CH_3OH}/K_{eq}\right)}{\left(1 + Af_{CO} + Bf_{H_2} + Cf_{CH_3OH} + Df_{CO_2}\right)^2}$$	cat: Cu containing $T \in 503 - 538\ [K]$ $P \in 8 - 14\ [MPa]$
Villa et al. (1985)	$$r_{CO\rightarrow CH_3OH} = \frac{f_{CO}f_{H_2}^2 - f_{CH_3OH}/K_2^*}{\left(A + Bf_{CO} + Cf_{H_2} + Gf_{CO_2}\right)^3}$$ $$r_{RWGS} = \frac{f_{CO_2}f_{H_2} - f_{CO}f_{H_2O}K_3^*}{M^2}$$	cat: $Cu\|ZnO\|Al_2O_3$ $T \in 488 - 518\ [K]$ $P \in 3 - 9.5\ [MPa]$
Graaf et al. (1988)	$$r_{CO\rightarrow CH_3OH} = \frac{k_1 K_{CO}\left(f_{CO}f_{H_2}^{1.5} - \frac{f_{CH_3OH}}{f_{H_2}^{0.5}K_1^{eq}}\right)}{1 + K_{CO}f_{CO} + K_{CO_2}f_{CO_2}\left(f_{H_2}^{0.5} + \left(K_{H_2O}/k_{H_2}^{0.5}\right)f_{H_2O}\right)}$$ $$r_{RWGS} = \frac{k_2 K_{CO_2}\left(f_{CO_2}f_{H_2} - \frac{f_{H_2O}f_{CO}}{K_2^{eq}}\right)}{1 + K_{CO}f_{CO} + K_{CO_2}f_{CO_2}\left(f_{H_2}^{0.5} + \left(K_{H_2O}/k_{H_2}^{0.5}\right)f_{H_2O}\right)}$$ $$r_{CO_2\rightarrow CH_3OH} = \frac{k_3 K_{CO_2}\left(f_{CO_2}f_{H_2}^{1.5} - \frac{f_{CH_3OH}f_{H_2O}}{f_{H_2}^{1.5}K_3^{eq}}\right)}{1 + K_{CO}f_{CO} + K_{CO_2}f_{CO_2}\left(f_{H_2}^{0.5} + \left(K_{H_2O}/k_{H_2}^{0.5}\right)f_{H_2O}\right)}$$	cat: $CuO\|ZnO\|Al_2O_3$ $T \in 483 - 563\ [K]$ $P \in 3 - 9\ [MPa]$
McNeil et al. (1989)	$$r_{CO_2\rightarrow CH_3OH} = k_1 K_{H_2}^2 K_{CO_2}\frac{p_{H_2}p_{CO_2} - \frac{p_{CO}p_{H_2O}}{K_{eq}^{r_{RWGS}}}}{\left(1 + K_{H_2}p_{H_2} + K_{CO_2}p_{CO_2} + K_{CH_3OH}p_{CH_3OH} + K_{H_2O}p_{H_2O} + K_{CO}p_{CO}\right)^3}$$	cat: $CuO\|ZnO\|Al_2O_3$ $T = 513\ [K]$ $P \in 2.89 - 4.38\ [MPa]$
Vanden Bussche and Froment (1996)	$$r_{CO_2\rightarrow CH_3OH} = \frac{k_{5a}'K_2'K_3K_4K_{H_2}p_{CO_2}p_{H_2}\left[1 - \left(\frac{1}{K^*}\right)\left(\frac{p_{H_2O}\cdot p_{CH_3OH}}{p_{CO_2}\cdot p_{H_2}^3}\right)\right]}{\left(1 + \left(\frac{K_{H_2O}}{K_8 K_9 K_{H_2}}\right)\left(\frac{p_{H_2O}}{p_{H_2}}\right) + \sqrt{K_{H_2}p_{H_2}} + K_{H_2O}p_{H_2O}\right)^3}$$ $$r_{RWGS} = \frac{k_1'p_{CO_2}\left[1 - K_3^*\left(\frac{p_{H_2O}p_{CO}}{p_{CO_2}p_{H_2}}\right)\right]}{1 + \left(\frac{K_{H_2O}}{K_8 K_9 K_{H_2}}\right)\left(\frac{p_{H_2O}}{p_{H_2}}\right) + \sqrt{K_{H_2}p_{H_2}} + K_{H_2O}p_{H_2O}}$$	cat: $CuO\|ZnO\|Al_2O_3$ $T \in 453 - 553\ [K]$ $P \in 1.5 - 5.1\ [MPa]$

Kubota et al. (2001)	$$r_{CO_2 \to CH_3OH} = \frac{k_M \left[\left(p_{CO_2}p_{H_2} - p_{CH_3OH}p_{H_2O}\right) \Big/ \left(K_M p_{H_2}^2\right) \right]}{\left(1 + K_{CO_2}p_{CO_2} + K_{H_2O}p_{H_2O}\right)^2}$$ $$r_{RWGS} = \frac{k_R \left[\left(p_{CO_2} - p_{CO}p_{H_2O}\right) \Big/ \left(K_R p_{H_2}\right) \right]}{\left(1 + K_{CO_2}p_{CO_2} + K_{H_2O}p_{H_2O}\right)}$$	cat: $Cu\|ZnO$ $T \in 473 - 548 \ [K]$ $P = 4.9 \ [MPa]$
Lim et al. (2009)	$$r_{CO \to CH_3OH} = \frac{k_{r_{CO \to CH_3OH}}K_{CO}K_{H_2}^2 K_{CH,CO}\left[p_{CO}p_{H_2}^{0.5} - p_{CH_3OH}/K_{r_{CO \to CH_3OH}}\right]}{\left(1 + K_{CO}p_{CO}\right)\left(1 + K_{H_2}^{0.5}p_{H_2}^{0.5} + K_{H_2O}p_{H_2O}\right)}$$ $$r_{RWGS} = \frac{k_{r_{RWGS}}K_{CO_2}K_{H_2}^2\left[p_{CO_2}p_{H_2} - p_{CO}p_{H_2O}/K_{r_{RWGS}}\right]}{\left(1 + K_{CO_2}p_{CO_2}\right)\left(1 + K_{H_2}^{0.5}p_{H_2}^{0.5} + K_{H_2O}p_{H_2O}\right)p_{H_2}^{0.5}}$$ $$r_{CO_2 \to CH_3OH} = \frac{k_{r_{CO_2 \to CH_3OH}}K_{CO_2}K_{H_2}K_{CH,CO}\left[p_{CO_2}p_{H_2}^3 - p_{H_2O}p_{CH_3OH}/K_{r_{CO_2 \to CH_3OH}}\right]}{\left(1 + K_{CO_2} \cdot p_{CO_2}\right)\left(1 + K_{H_2}^{0.5} \cdot p_{H_2}^{0.5} + K_{H_2O} \cdot p_{H_2O}\right)p_{H_2}^{0.5}}$$	cat: $CuO\|ZnO\|Al_2O_3\|ZrO_2$ $T \in 523 - 553 \ [K]$ $P = 5 \ [MPa]$
Park et al. (2014)	$$r_{CO \to CH_3OH} = \frac{k'_{r_{CO \to CH_3OH}}K_{CO}\left[f_{CO}f_{H_2}^{0.5} - f_{CH_3OH}/\left(f_{H_2}^{0.5} \cdot K_{r_{CO \to CH_3OH}}\right)\right]}{\left(1 + K_{CO}f_{CO}\right)\left(1 + K_{H_2}^{0.5}f_{H_2}^{0.5} + K_{H_2O}f_{H_2O}\right)}$$ $$r_{RWGS} = -\frac{k'_{r_{RWGS}}K_{CO_2}\left[f_{CO_2}f_{H_2} - f_{CO}f_{H_2O}/K_{r_{RWGS}}\right]}{\left(1 + K_{CO}f_{CO_2}\right)\left(1 + K_{H_2}^{0.5}f_{H_2}^{0.5} + K_{H_2O}f_{H_2O}\right)}$$ $$r_{CO_2 \to CH_3OH} = \frac{k'_{r_{CO_2 \to CH_3OH}}K_{CO_2}\left[f_{CO_2}f_{H_2}^{0.5} - f_{H_2O}f_{CH_3OH}/\left(f_{H_2}^{1.5}K_{r_{CO_2 \to CH_3OH}}\right)\right]}{\left(1 + K_{CO_2}f_{CO_2}\right)\left(1 + K_{H_2}^{0.5}f_{H_2}^{0.5} + K_{H_2O}f_{H_2O}\right)}$$	cat: $Cu\|ZnO\|Al_2O_3$ $T \in 493 - 613 \ [K]$ $P \in 50 - 90 \ [bar]$

Table 3.2: Equation rates for methanol synthesis

(Natta, 1955; Bakemeier, Laurer and Schroeder, 1970; Leonov *et al.*, 1973; Schermuly and Luft, 1977; Klier *et al.*, 1982; Seyfert and Luft, 1985; Villa *et al.*, 1985; Graaf, Stamhuis and Beenackers, 1988; McNeil, Schack and Rinker, 1989; Vanden Bussche and Froment, 1996; Kubota *et al.*, 2001; Lim *et al.*, 2009; Park, Park, *et al.*, 2014)

3.3 Reactor model and parameter estimation

The experimental data was obtained in an integral reactor, therefore, require integration of the conservation equations over the reactor.

Following Young and Finlayson work for a criterion for neglecting axial dispersion on packed bed chemical reactors (Young and Finlayson, 1973) together with Mears parameter to evaluate the contribution of external mass diffusion (Mears, 1971). A pseudohomogeneous one-dimensional plug-flow reactor model was applied (Froment, De Wilde and Bischoff, 2011). Due to the fact that the isothermal profile was determined experimentally, integration of the energy equation was not necessary, while the pressure drop was also considered negligible.

The estimation of the parameters was based on minimizing the objective function $\left(F_{obj}\right)$ and the residuals of square errors of the objective elements (CO and CO_2 outlet molar flows), expressed as follows:

$$F_{obj} = \sum_n^{NE}\left[\sum_i w_i\left(\frac{X_{i,calc} - X_{i,exp}}{X_{i,exp}}\right)^2\right]_n \qquad \textit{Eq. 3.1}$$

The estimation was conducted using the "LeastSquareAnalysis" tool from the BzzMath library (Buzzi-Ferraris and Manenti, 2012). Thanks to the availability of Park's data on his publication, an algorithm validation was performed by following the parametrization process obtaining similar results.

3.4 Results and discussion

In the following sections is presented a summary of the parameters obtained for the three models for both catalysts and a comparison to the value published by each author.

The equilibrium constants for the three models were extracted from Graaf's work on methanol synthesis equilibrium (Graaf *et al.*, 1986). None of the parameters from those expressions were considered in the reparametrization process, same decision taken by the three model authors, as they showed little effect on the reaction rates.

Vanden's model

The model was restructured so it allowed working with feed in the absence of CO_2 since the form presented in Eq. 2.20 and Eq. 2.21 gets indeterminate in those cases.

$$r_{CO_2 \rightarrow CH_3OH} = \frac{c_4 p_{H_2} \left[p_{CO_2} - \left(\frac{1}{K_{CO_2}^{eq}} \right) \left(\frac{p_{H_2O} \cdot p_{CH_3OH}}{p_{H_2}^3} \right) \right]}{\left(1 + c_3 \left(\frac{p_{H_2O}}{p_{H_2}} \right) + c_1 \sqrt{p_{H_2}} + c_2 p_{H_2O} \right)^3} \qquad Eq.\ 3.2$$

$$r_{RWGS} = \frac{c_5 \left[p_{CO_2} - K_{RWGS}^{eq} \left(\frac{p_{H_2O} p_{CO}}{p_{H_2}} \right) \right]}{1 + c_3 \left(\frac{p_{H_2O}}{p_{H_2}} \right) + c_1 \sqrt{p_{H_2}} + c_2 p_{H_2O}} \qquad Eq.\ 3.3$$

where the values for K_1^* and K_3^* are:

$$\log_{10} \left(K_{CO_2}^{eq} \right) = \frac{3066}{T} - 10.592 \qquad Eq.\ 3.4$$

$$\log_{10} \left(\frac{1}{K_{RWGS}^{eq}} \right) = \frac{-2073}{T} + 2.029 \qquad Eq.\ 3.5$$

The results of the reparametrization process for the Vanden model are summarized in the following table.

Coeff.	Original	Estimated CZA synth	Estimated CZA comm
c_1	$0.499 \cdot \exp\left(\dfrac{17197}{RT}\right)$	$0.644 \cdot \exp\left(\dfrac{21719}{RT}\right)$	$0.376 \cdot \exp\left(\dfrac{23183}{RT}\right)$
c_2	$(6.62 \cdot 10^{-11}) \cdot \exp\left(\dfrac{124119}{RT}\right)$	$(3.31 \cdot 10^{-7}) \cdot \exp\left(\dfrac{96829}{RT}\right)$	$(3.31 \cdot 10^{-7}) \cdot \exp\left(\dfrac{88741}{RT}\right)$
c_3	3453.38	1064.90	2716.61
c_4	$1.07 \cdot \exp\left(\dfrac{36696}{RT}\right)$	$1.82 \cdot \exp\left(\dfrac{47966}{RT}\right)$	$1.37 \cdot \exp\left(\dfrac{44834}{RT}\right)$
c_5	$(1.22 \cdot 10^{10}) \cdot \exp\left(\dfrac{-94765}{RT}\right)$	$(5.90 \cdot 10^{9}) \cdot \exp\left(\dfrac{-48144}{RT}\right)$	$(1.88 \cdot 10^{10}) \cdot \exp\left(\dfrac{-70605}{RT}\right)$

Table 3.3: Original and estimated parameters for Vanden's model

The denominator on both reaction rate expressions (Eq. 3.2 and Eq. 3.3) represents the reciprocal of the ratio between the concentration of free active sites (c_s) and the total number of sites (c_t) (Vanden Bussche and Froment, 1996).

$$\beta = \frac{c_s}{c_t} = \frac{1}{1 + c_3\left(\dfrac{p_{H_2O}}{p_{H_2}}\right) + c_1\sqrt{p_{H_2}} + c_2 p_{H_2O}}$$

Eq. 3.6

Figure 3.3 shows the relative error for every run of experiment molar for both the CO (section A) and CO_2 (section B) molar flowrate at the reactor's outlet.
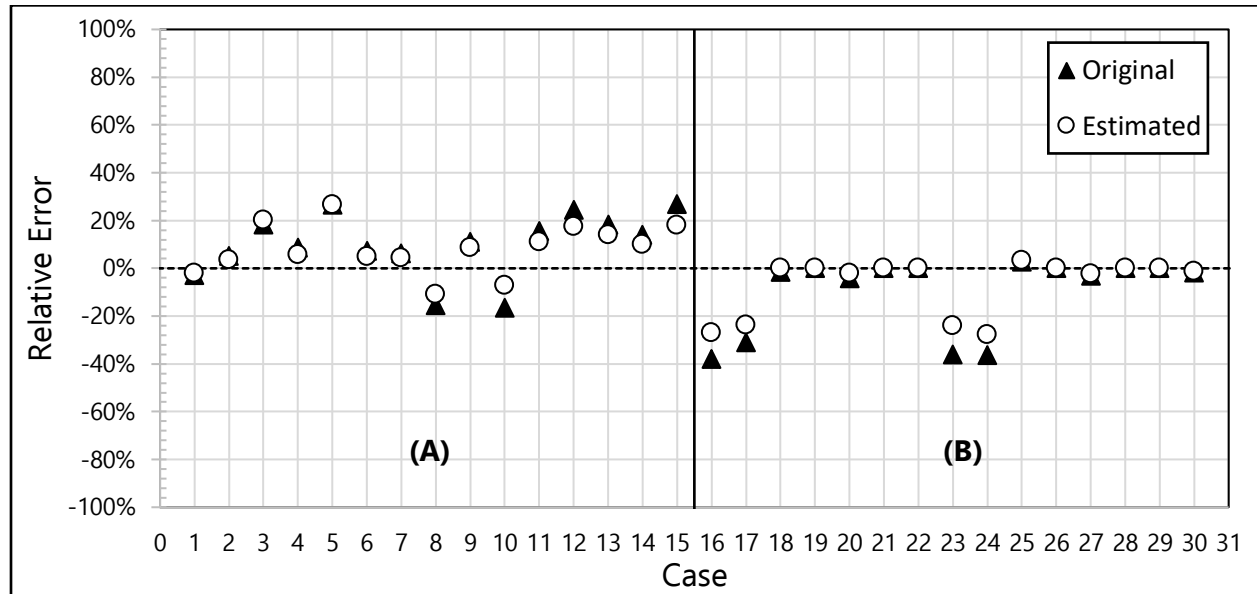

Figure 3.3: Relative errors for every individual experimental run using the Vanden model. (A) Molar flowrate of CO exiting the reactor, (B) Molar flowrate of CO_2 exiting the reactor

The mean relative error for the original and estimated Vanden's model reached a value of 0.90 and 0.52 respectively for the whole batch of experiments under the synthesize catalyst. The reparametrization model adds an overall improvement over the original model. Most cases

showed a relative error not greater than 2% with their respective original value. In cases where the model struggles to present a good representation of the experimental results, the operative conditions were "extreme" and far away from the expected conditions in real plants by having the absent or notably low concentrations of CO_x in the feed (cases 3, 5, 16, 17, 23 and 24), compositions that are not feasible to reach on a real plant scenario considering the water gas shift reaction progressing towards equilibrium in combination to the presence of a recycle stream in methanol synthesis plants.

Graaf's model

$$r_{CO \to CH_3OH} = \frac{c_1 c_4 \left(f_{CO} f_{H_2}^{1.5} - \frac{f_{CH_3OH}}{f_{H_2}^{0.5} K_{CO}^{eq}} \right)}{1 + c_4 f_{CO} + c_5 f_{CO_2} \left(f_{H_2}^{0.5} + c_6 f_{H_2O} \right)}$$

Eq. 3.7

$$r_{RWGS} = \frac{c_2 c_5 \left(f_{CO_2} f_{H_2} - \frac{f_{H_2O} f_{CO}}{K_{RWGS}^{eq}} \right)}{1 + c_4 f_{CO} + c_5 f_{CO_2} \left(f_{H_2}^{0.5} + c_6 f_{H_2O} \right)}$$

Eq. 3.8

$$r_{CO_2 \to CH_3OH} = \frac{c_3 c_5 \left(f_{CO_2} f_{H_2}^{1.5} - \frac{f_{CH_3OH} f_{H_2O}}{f_{H_2}^{1.5} K_{CO_2}^{eq}} \right)}{1 + c_4 f_{CO} + c_5 f_{CO_2} \left(f_{H_2}^{0.5} + c_6 f_{H_2O} \right)}$$

Eq. 3.9

Since two of the three reaction rates are independent from a thermodynamic standpoint, K_{CO}^{eq} can be calculated from a linear combination of the other equilibrium constant values (Eq. 3.4 and Eq. 3.5), hence:

$$\log_{10}\left(K_{CO}^{eq} \right) = \frac{5139}{T} - 12.621$$

Eq. 3.10

The results of the reparametrization process for the Graaf model are summarized in the following table.

Coeff.	Original	Estimated CZA synth	Estimated CZA comm
c_1	$(2.69 \cdot 10^7) \cdot \exp\left(\frac{-109900}{RT}\right)$	$(1.46 \cdot 10^7) \cdot \exp\left(\frac{-113572}{RT}\right)$	$(6.47 \cdot 10^7) \cdot \exp\left(\frac{-120314}{RT}\right)$
c_2	$(7.31 \cdot 10^8) \cdot \exp\left(\frac{-123000}{RT}\right)$	$(1.96 \cdot 10^9) \cdot \exp\left(\frac{-189348}{RT}\right)$	$(2.26 \cdot 10^{10}) \cdot \exp\left(\frac{-292083}{RT}\right)$
c_3	$(4.36 \cdot 10^2) \cdot \exp\left(\frac{-65200}{RT}\right)$	$(1.12 \cdot 10^3) \cdot \exp\left(\frac{-87.57}{RT}\right)$	$(6.24 \cdot 10^3) \cdot \exp\left(\frac{-47600}{RT}\right)$
c_4	$(7.99 \cdot 10^{-7}) \cdot \exp\left(\frac{58100}{RT}\right)$	$(4.87 \cdot 10^{-2}) \cdot \exp\left(\frac{86017}{RT}\right)$	$(7.62 \cdot 10^{-2}) \cdot \exp\left(\frac{64162}{RT}\right)$
c_5	$(1.02 \cdot 10^{-7}) \cdot \exp\left(\frac{67400}{RT}\right)$	$(1.04 \cdot 10^{-2}) \cdot \exp\left(\frac{31623}{RT}\right)$	$(1.01 \cdot 10^{-2}) \cdot \exp\left(\frac{33224}{RT}\right)$
c_6	$(4.13 \cdot 10^{-11}) \cdot \exp\left(\frac{104500}{RT}\right)$	$(2.90 \cdot 10^{-5}) \cdot \exp\left(\frac{9.32}{RT}\right)$	$(2.21 \cdot 10^{-6}) \cdot \exp\left(\frac{67795}{RT}\right)$

Table 3.4: Original and estimated parameters for Graaf's model

As in the Vanden model, the denominator for the three reaction rates represents the reciprocal for the ratio between the concentration of free active sites (c_s) and the total number of sites (c_t).

$$\beta = \frac{c_S}{c_t} = \frac{1}{1 + c_4 f_{CO} + c_5 f_{CO_2}\left(f_{H_2}^{0.5} + c_6 f_{H_2O}\right)} \qquad \textit{Eq. 3.11}$$

Figure 3.4 shows the relative error for every run of experiment for both the original and estimated parameters.
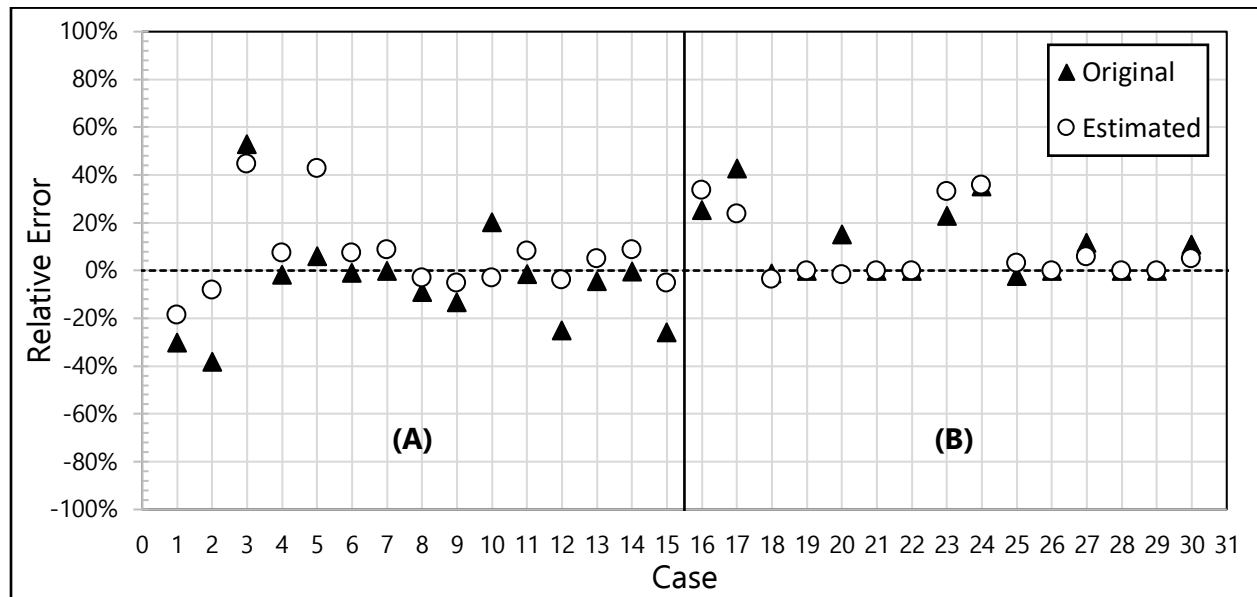

Figure 3.4: Relative errors for every individual experimental run using the Graaf model. (A) Molar flowrate of CO exiting the reactor, (B) Molar flowrate of CO₂ exiting the reactor

The mean relative error for the original and estimated Graaf's model reached a value of 1.05 and 0.89 respectively for the whole batch of experiments. The estimated parameters model shows little overall improvement over the original model and as Vanden model, it shows a struggle to make an authentic representation of the results for feeds with absent or low composition of CO_x.

[_Explain bad values_]

Even with the new estimated parameters, Graaf's model does not represent the kinetics for methanol synthesis as good as Vanden's model. Redoing the model discrimination by following Graaf's procedure can improve the final accuracy of the model by attempting different driving forces on the kinetic expression according to the multiple rate determining steps options under consideration.

Park's model

$$r_{CO \to CH_3OH} = \frac{c_1 K_{CO}\left[f_{CO}f_{H_2}^{0.5} - f_{CH_3OH}/\left(f_{H_2}^{0.5} \cdot K_{r_{CO \to CH_3OH}}\right)\right]}{\left(1 + K_{CO}f_{CO}\right)\left(1 + K_{H_2}^{0.5}f_{H_2}^{0.5} + c_4 f_{H_2O}\right)}$$

Eq. 3.12

$$r_{RWGS} = -\frac{c_2 K_{CO_2}\left[f_{CO_2}f_{H_2} - f_{CO}f_{H_2O}/K_{r_{RWGS}}\right]}{\left(1 + K_{CO}f_{CO_2}\right)\left(1 + K_{H_2}^{0.5}f_{H_2}^{0.5} + c_4 f_{H_2O}\right)}$$

Eq. 3.13

$$r_{CO_2 \to CH_3OH} = \frac{c_3 K_{CO_2}\left[f_{CO_2}f_{H_2}^{0.5} - f_{H_2O}f_{CH_3OH}/\left(f_{H_2}^{1.5} K_{r_{CO_2 \to CH_3OH}}\right)\right]}{\left(1 + K_{CO_2}f_{CO_2}\right)\left(1 + K_{H_2}^{0.5}f_{H_2}^{0.5} + c_4 f_{H_2O}\right)}$$

Eq. 3.14

Like the previous models, the equilibrium constants were fetched from Graff (Graaf *et al.*, 1986) and Ng (Ng, Chadwick and Toseland, 1999) work.

The results of the reparametrization process for the Park's model are summarized in the following table.

Coeff.	Original	Estimated CZA synth	Estimated CZA comm
c_1	$(1.88 \cdot 10^8) \cdot \exp\left(\frac{-113711}{RT}\right)$	$(7.32 \cdot 10^{10}) \cdot \exp\left(\frac{-121337}{RT}\right)$	$(1.82 \cdot 10^8) \cdot \exp\left(\frac{-113434}{RT}\right)$
c_2	$(1.16 \cdot 10^{10}) \cdot \exp\left(\frac{-126573}{RT}\right)$	$(7.47 \cdot 10^6) \cdot \exp\left(\frac{-82267}{RT}\right)$	$(7.47 \cdot 10^6) \cdot \exp\left(\frac{-82267}{RT}\right)$
c_3	$(7.08 \cdot 10^4) \cdot \exp\left(\frac{-68252}{RT}\right)$	$(6.30 \cdot 10^7) \cdot \exp\left(\frac{-89019}{RT}\right)$	$(6.79 \cdot 10^4) \cdot \exp\left(\frac{-71645}{RT}\right)$
c_4	$(3.80 \cdot 10^{-10}) \cdot \exp\left(\frac{80876}{RT}\right)$	$(8.72 \cdot 10^{-2}) \cdot \exp\left(\frac{52157}{RT}\right)$	$(2.70 \cdot 10^{-5}) \cdot \exp\left(\frac{78268}{RT}\right)$

Table 3.5: Original and estimated parameters for Park's model

Figure 3.5 shows the relative error for every run of experiment for both the original and estimated parameters.

The mean relative error for the original and estimated Park's model reached a value of 2.43 and 1.35 respectively for the whole batch of experiments. The estimated parameters model shows an overall improvement over the original model with the same problem observed on previous models for "extremist" feeds. Overall, Park's model showed the worst representation for the process, this result can be interpreted as having a process which doesn't follow Park's three site kinetic model.
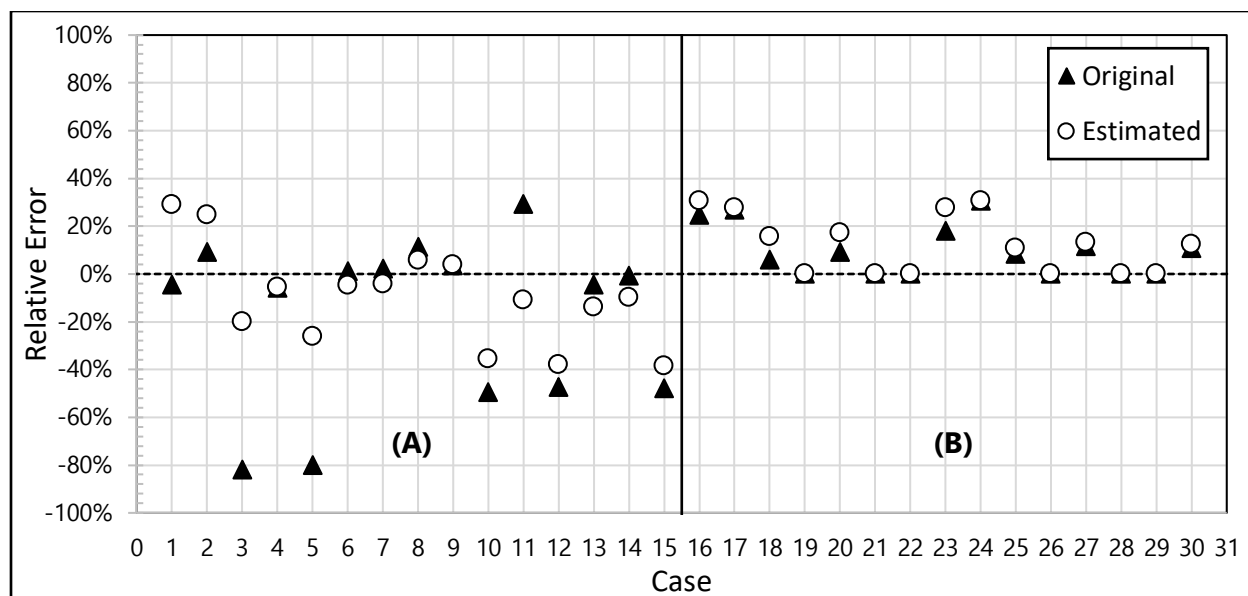
Figure 3.5: Relative errors for every individual experimental run using the Park model. (A) Molar flowrate of CO exiting the reactor, (B) Molar flowrate of CO_2 exiting the reactor

Overall, Vanden's personalized model has shown to best describe the reaction involved in methanol synthesis for both the synthesized and the commercial CZA catalyst. Even showing better results compared to similar studies (Lim *et al.*, 2009). The cases were the model struggles to present a good representation of the kinetics are found to be at conditions not expected to utilize at real plants with a recycle stream.

It's also the computational lightest of the three models, allowing fast computational simulations. For these reasons, it became the chosen model for the sensitivity analysis and the subsequent plant simulation.

It should be noticed that, although the reparametrization of the model developed in the present study is based on the intrinsic kinetics, its application is limited to catalyst with similar composition and characterization, this is attributable to the fact that different composition may have different RDS as discussed in the introduction section

3.4.1   Sensitivity analysis

A study has been performed to determine the effects of temperature, CO ratio (Eq. 3.15), and S (Eq. 2.5) values over the hydrogenation and WGS instant and accumulated reaction rates over the reactor.

$$CO\ ratio = \frac{moles\ CO}{molar\ CO + moles\ CO_2}$$ *Eq. 3.15*

It is recommended to take special care examining the results below, in consequence of the nature of the three-dimensional plot, some graphs have been rotated to show a better angle of the results. The reactor length axis has been normalized.

Temperature effect

A set of reactor simulations were performed with a temperature range from 230 to 270°C, a feed composition of H_2, CO, CO_2 and N_2 equal to 0.65, 0.20, 0.05 and 0.10 respectively, at a pressure of 20 bars and space velocity (SV) of 6040 $\left[\frac{mL}{gCat. \cdot h}\right]$.

Both reaction rates have extreme cases at the inlet of the reactor (Figure 3.6 and Figure 3.7), this is because of the absence of methanol and water which displace the equilibrium to the right side for the hydrogenation and to the left side for the water gas shift reaction. This effect is quickly stabilized once more of these substances are produced. As this happens, we observe a change of direction for the water gas shift reaction, it starts consuming CO and water to produce H_2 and CO_2.
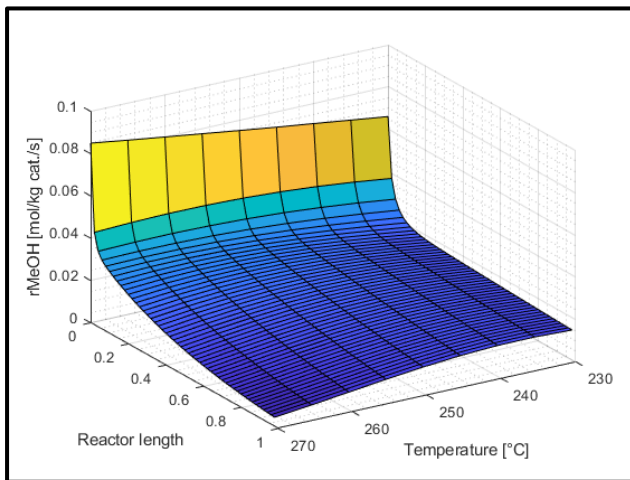

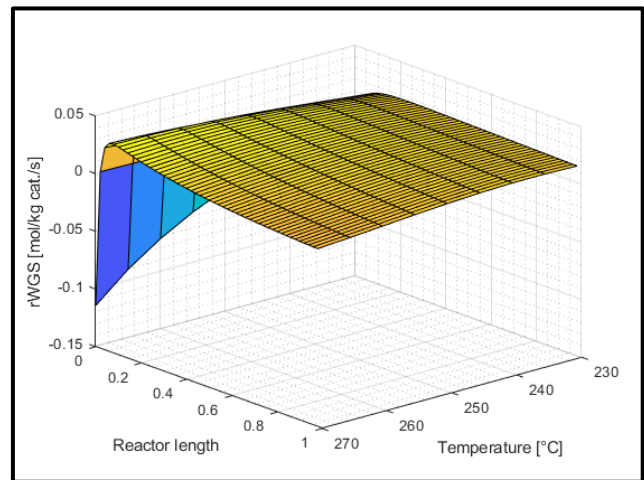Figure 3.6: Effect of temperature over the rMeOH along the reactor

Figure 3.7: Effect of temperature over the rWGS along the reactor

Figure 3.8 shows the accumulated methanol synthesis reaction rate along the reactor for different temperatures, the solid line shows the optimal temperature for the current reactor length, 245°C. The red circles along the surface plot depicts the maximum value at different lengths inside the reactor, is noticeable a shift in the maximum value along the reactor.

A similar case is observed in Figure 3.9 for the accumulated WGS reaction, the maximum is reached at the same temperature of 245°C. More interesting, a shift into equilibrium can be observed by the displacement of the maximum value along the reactor depicted by the red circles.
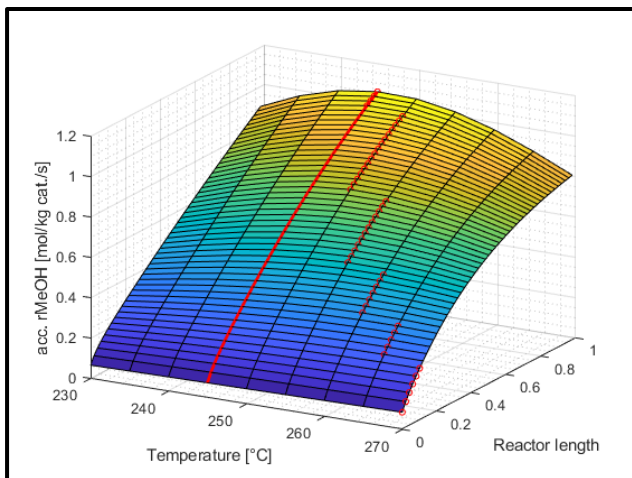
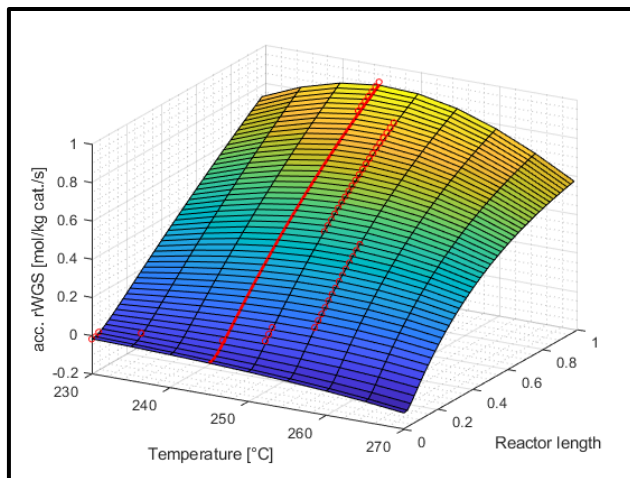*Figure 3.8: Effect of temperature over the accumulated rMeOH along the reactor*

Figure 3.9: Effect of temperature over the accumulated rWGS along the reactor

Overall, the WGS reaction presents the advantage of "refilling" the reagent for the CO_2 hydrogenation reaction by producing H_2 and CO_2, assuring a level of CO_2 along the reactor. This can be seen in Figure 3.11. At the feed, the WGS reaction goes backwards consuming CO_2, but as both reaction advance, the change of direction for the WGS reaction help maintaining a steady level of CO_2 conversion around 4-6%.

On the other hand, the presence of the WGS reaction makes it difficult for the use of a higher concentration of CO_2 at the feed. This will displace the equilibrium to the left, consuming H_2 and producing H_2O along the way, both effects sharing the same consequence of reducing the hydrogenation reaction rate.
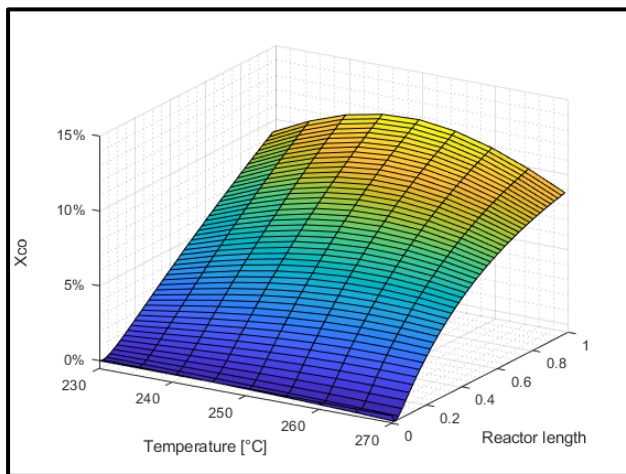

Figure 3.10: Effect of temperature over the carbon monoxide conversion along the reactor
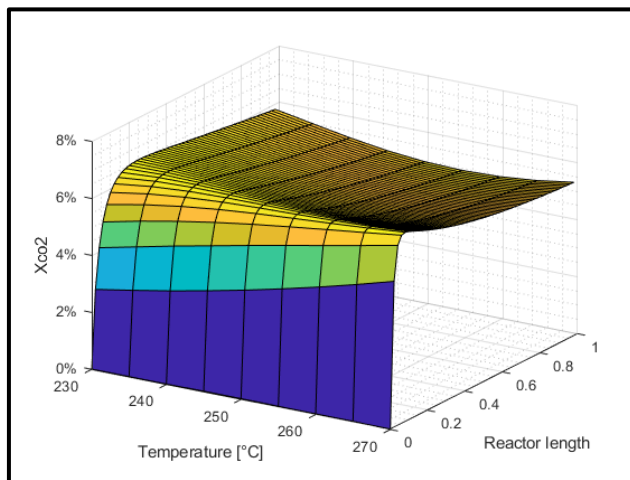

Figure 3.11: Effect of temperature over the carbon dioxide conversion along the reactor

To answer the question of how much CO_2 should be at the feed in order to maximize the methanol production and maintaining the forward direction for the WGS reaction, a sensitivity analysis was performed for the effect of CO ratio.

CO ratio effect

A set of reactor simulations were performed with a CO ratio range from 0.05 to 0.95, a feed composition of H_2, $CO + CO_2$ and N_2 equal to 0.67, 0.235 and 0.095 respectively; a SV of 6040 $\left[\frac{mL}{g\ cat.\ \cdot\ h}\right]$ at a reactor temperature of 245°C and 20 bars of pressure.

Figure 3.12 and Figure 3.13 display the effect of CO ratio over the hydrogenation and the water gas shift reaction rates along the reactor. The red circles show the position along the reactor for the maximum reaction rates for the hydrogenation and WGS reactions. It is essential to notice that a feed with high concentration of CO_2 – low CO ratio – ensures a high reaction rates for the hydrogenation rate only at the beginning of the reactor, past the initial part, higher rates are observed for feed with higher concentrations of CO instead. On the same topic, the WGS reaction displays negative values for most of the reactor length for feeds with high CO_2 concentrations. This confirms the importance of having a feed that assures a forward direction for the WGS reaction and sets the hydrogenation reaction as a consecutive reaction, not as a competitive one.
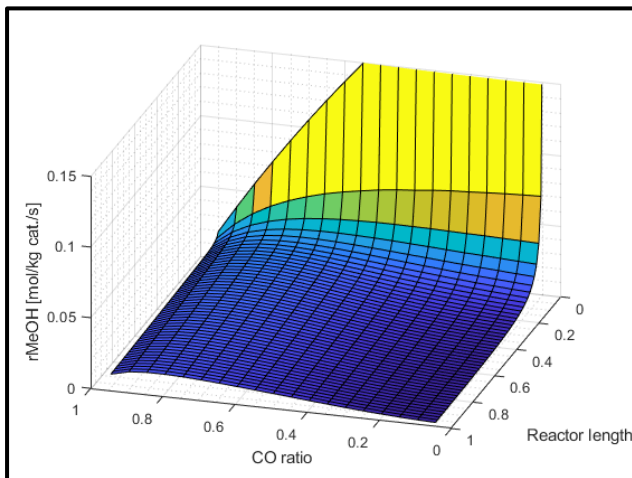

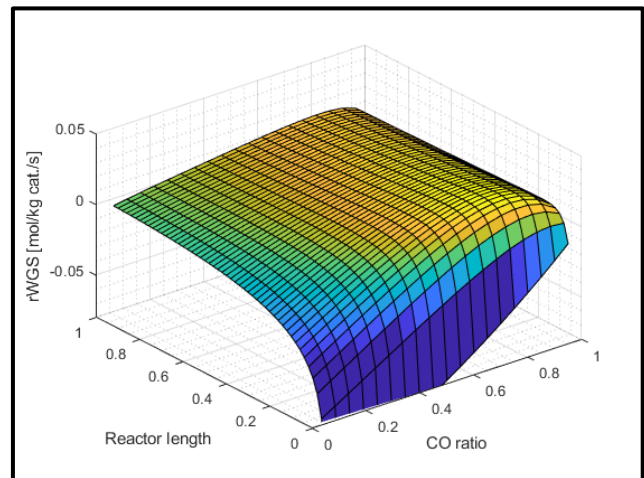*Figure 3.12: Effect of CO ratio over the rMeOH along the reactor*

Figure 3.13: Effect of CO ratio over the rWGS along the reactor

Figure 3.14 shows the accumulated methanol synthesis reaction rate along the reactor for different values of CO ratio. The optimal value for CO ratio that maximize the accumulated hydrogenation is 0.75 (S value equal to 2.60 under those compositions). Similar to the effect of temperature, the optimal value of CO ratio that maximize the methanol production changes depending on the reactor's length (and more concrete, the gas space velocity), these values are represented by the circle marks along the surface plot.

A similar observation can be done in Figure 3.15 for the accumulated WGS reaction rate along the reactor. A value of 0.8 for the CO ratio presents the maximum path (S value of 2.65 under those compositions), a positive value, meaning the overall reaction is proceeding in the forward direction producing H_2 and CO_2, both of which are consecutively consumed by the hydrogenation reaction producing methanol.
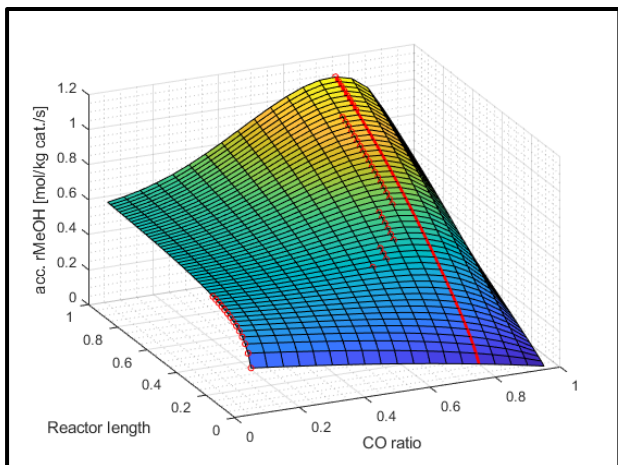
Figure 3.14: Effect of CO ratio over the accumulated rMeOH along the reactor

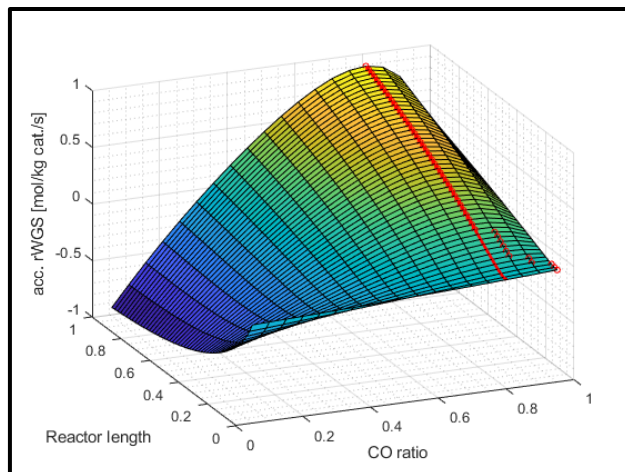Figure 3.15: Effect of CO ratio over the accumulated rWGS along the reactor

The CO and CO_2 conversion behave as expected; if the feed has a CO ratio low enough, the WGS reaction does not present a direction shift for most of the reactor's length, this is observed as high values for the CO_2 conversion (consumed on both reactions) along negative values for the CO conversion (not consumed but produced by the WGS reaction). For feeds with high CO ratio values, the conversion of CO shows positive values, related to being consumed by the forward direction of the WGS, and a CO_2 conversion that increases at the first instances of the reactor but then it reaches a plateau, this is mostly explained by absent of methanol and water at the feed which displaces the equilibrium, consuming CO_2, but once a convenient amount of water is produced, the WGS shift directions replenishing the amount of CO_2 being consumed by the hydrogenation reaction.
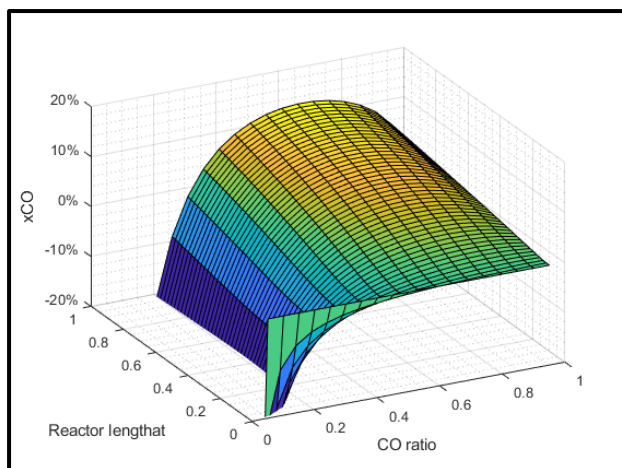
Figure 3.16: Effect of CO ratio over the carbon monoxide conversion along the reactor
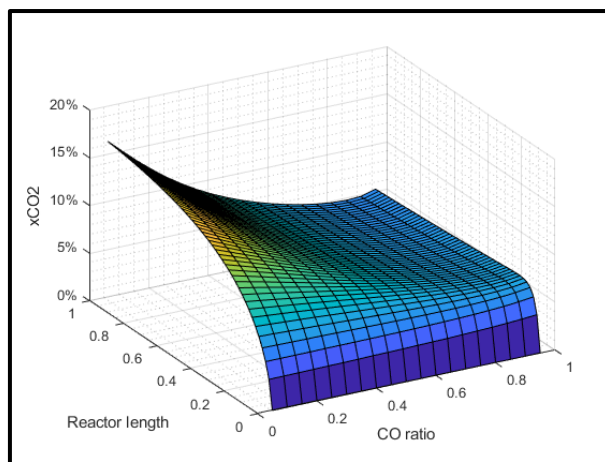
Figure 3.17: Effect of CO ratio over the carbon dioxide conversion along the reactor

These result give a good understanding of the phenomena involved in the methanol synthesis, however, since the conversion per pass is limited by the thermodynamic equilibrium limit, a recycle

stream must be present on a methanol synthesis plant to be able to increase the methanol overall yield. Under this case, a proper plant simulation study should be performed.

Chapter 4:
Steady state plant simulation

A steady state plant simulation was performed to study the key performance indicators for the methanol synthesis from syngas. PRO II v9.1 was employed to simulate a plant with a recycle stream to study the optimization of the plant configuration to maximize methanol production whilst maintaining a feasible recycle ratio.

4.1   Reactor Characteristics

An isothermal plug flow reactor was chosen as a model reactor for the conversion of syngas into methanol applying the Vanden model with custom coefficients for the simulation of the reaction rates. The fugacity of compound involved were calculated using Soave-Redlinch-Kwong equation of state (Soave, 1972).

A base case was built from plant design and reactor configurations available in the literature (Arab *et al.*, 2014; Park, Kim, *et al.*, 2014; Kiss *et al.*, 2016; Rsiveras-Tinoco *et al.*, 2016; Szima and Cormos, 2018).

Algorithm 4.1 presents the kinetic procedure implemented in PROII utilizing Vanden's model with custom coefficients.

4.2   MeOH plant simulation

Methanol synthesis follows the typical reaction-separation-recycle system. Conversions are incomplete due to the presence of limiting chemical equilibrium, because of this, the outlet of the reactor will comprise of products (methanol and water) as well as unconverted reactants (CO_x and hydrogen). The gaseous mixture is cooled and flashed to separate the condensable products from the non-condensable reactants, which are recycled back to the reactor.

In this work, a feed of 1500 [kgmol/h] is considered for every run of the simulation, common feed for methanol plants with a capacity of 100 [ktpy]. Figure 4.1 presents the proposed flowsheet while a more complete mass and energy balance for the optimal configuration is present in Table 4.1. There was a lack of inerts considered in the present study as a way to focus on the core phenomena of methanol synthesis.
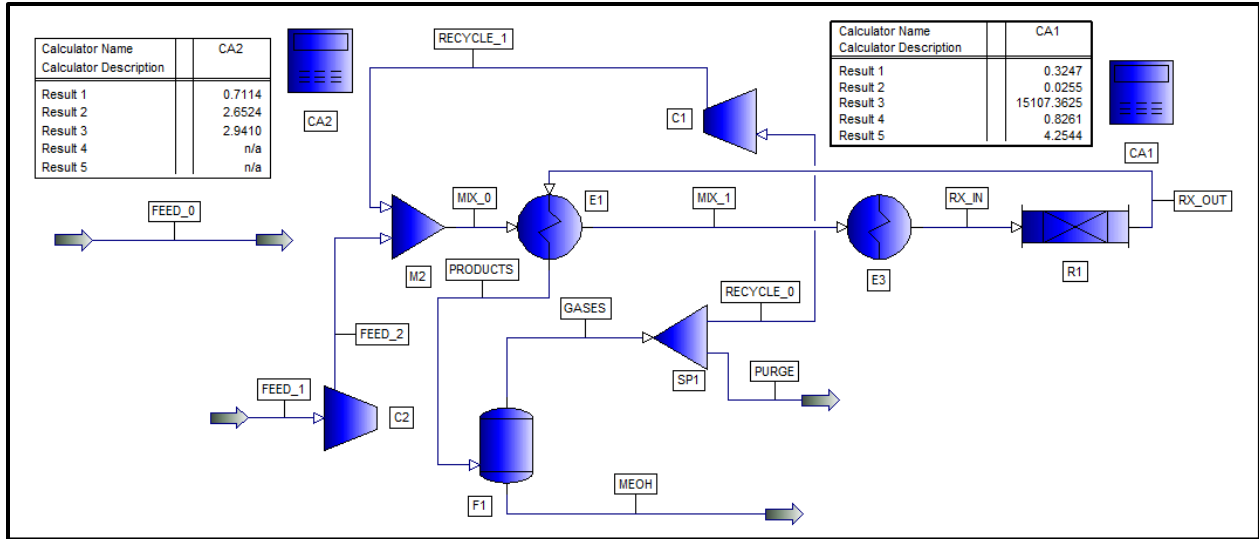
Figure 4.1: ProII flowsheet of an methanol synthesis synthesis by CO_2 hydrogenation

Stream Name	FEED_1	FEED_2	MIX_0	MIX_1	RX_IN	RX_OUT
Temperature [K]	298.000	840.338	411.476	500.000	503.150	503.150
Pressure [bar]	1.000	20.000	20.000	20.000	20.000	20.000
Phase	Vapor	Vapor	Vapor	Vapor	Vapor	Vapor
Flowrate [kgmol/h]	1500.000	1500.000	7881.672	7881.672	7881.672	6937.411
Flowrate [kg/h]	16202.81	16202.810	78632.598	78632.598	78632.598	78632.598
Flowrate [m³/h]	37179.085	5270.953	13582.419	16504.790	16608.601	14594.574
Enthalpy [kJ/kg]	101.087	1606.317	540.266	813.103	822.860	1003.838
Composition						
H_2	0.672	0.672	0.739	0.739	0.739	0.701
CO	0.312	0.312	0.179	0.179	0.179	0.137
CO_2	0.016	0.016	0.073	0.073	0.073	0.080
H_2O	0.000	0.000	0.002	0.002	0.002	0.004
CH_3OH	0.000	0.000	0.008	0.008	0.008	0.077
Stream Name	PRODUCTS	MEOH	GASES	PURGE	RECYCLE_0	RECYCLE_1
Temperature [K]	409.088	300.000	300.000	300.000	300.000	311.965
Pressure [bar]	20.000	18.000	18.000	18.000	18.000	18.000
Phase	Vapor	Mixed	Vapor	Vapor	Vapor	Vapor
Flowrate [kgmol/h]	6937.411	491.079	6446.333	64.463	6381.869	6381.869
Flowrate [kg/h]	78632.598	15572.195	63060.403	630.604	62429.799	62429.799
Flowrate [m³/h]	11842.555	19.442	8966.361	89.664	8876.697	8316.692
Enthalpy [kJ/kg]	731.004	-49.416	227.079	227.079	227.079	263.588
Composition						
H_2	0.701	0.001	0.755	0.755	0.755	0.755
CO	0.137	0.000	0.148	0.148	0.148	0.148
CO_2	0.080	0.009	0.086	0.086	0.086	0.086
H_2O	0.004	0.029	0.002	0.002	0.002	0.002
CH_3OH	0.077	0.960	0.010	0.010	0.010	0.010

Table 4.1: Mass and energy balance of the proposed methanol synthesis process

```
    R=8.314

    C1=0.644*EXP(21719/R/RTABS)
    C2=(3.31E-7)*EXP(96829/R/RTABS)
    C3=1064.90
    C4=1.82*EXP(47966/R/RTABS)
    C5=(5.90E9)*EXP(-48144/R/RTABS)

    K1=10**((3066/RTABS)-5.592)
    K3=1/(10**((-2073/RTABS)+2.029))

    PH2=RPRES*XVAP(1)
    PCO=RPRES*XVAP(2)
    PCO2=RPRES*XVAP(3)
    PCH3OH=RPRES*XVAP(5)
    PH2O=RPRES*XVAP(6)

    BETA=(1/(1+C3*(PH2O/PH2)+C1*SQRT(PH2)+C2*PH2O))

    UNITS=3600*1.775

    RRATES(1)=C4*PH2*(PCO2-(100000/K1)*PH2O*PCH3OH/(PH2**3))*(BETA**3)*UNITS
    RRATES(2)=C5*(PCO2-K3*((PH2O*PCO)/PH2))*BETA*UNITS
    RRATES(3)=-C5*(PCO2-K3*((PH2O*PCO)/PH2))*BETA*UNITS

    ISOLVE=1
    RETURN
```
Algorithm 4.1: Kinetic procedure implemented in PROII

4.3 Sensitivity analysis

A reactor length of $8\ [m]$ an inside diameter of $60\ [mm]$ and a total of 410 tubes was chosen as the base design, only changed for the gas hourly space velocity (GHSV) sensitivity analysis study adjusting it so the gas velocity does not exceeded 1.5 m/s. A value of 0.99 for the recycle split was selected. The following parameters were varied in the specified range: temperature = 220-270 °C, P = 20 bar, S = 1.4-2.6, CO ratio = 0.05-0.995. The temperature and pressure correspond to the value inside the reactor, while the S and CO ratio values correspond to the plant battery feed before the mixing with the recycle (stream FEED_2).

The optimal plant configuration should be able to maximize the methanol production outlet without compromising the amount of recycle the plant need to manage as it will affect negatively the overall CAPEX and OPEX of the plant. In the following analysis, the amount of recycle compared to the amount of feed to the plant is represented by:

$$Rrecycle = \frac{molar\ flow\ recycle\ stream}{molar\ flow\ feed\ stream}$$

Eq. 4.1

Temperature Effect

The following results were obtained for simulation runs with an CO ratio value set at 0.75 for the plant feed.

Methanol production shows a maximum value for a reactor temperature = 220°C and a feed with S = 1.7 (Figure 4.2) having neighbor points that maintain a close value to this maximum. Rrecycle shows a minimum value of 6.68 for a plant feed S value of 1.9 and at a reactor temperature of 230°C (Figure 4.3).

On Figure 4.4 is presented the ratio between the methanol production and the Rrecycle showing a clear maximum at a reactor's temperature of 230°C and a S value of 1.9. The S and CO ratio values at the reactor feed are equal to 1.5 and 0.41 respectively.
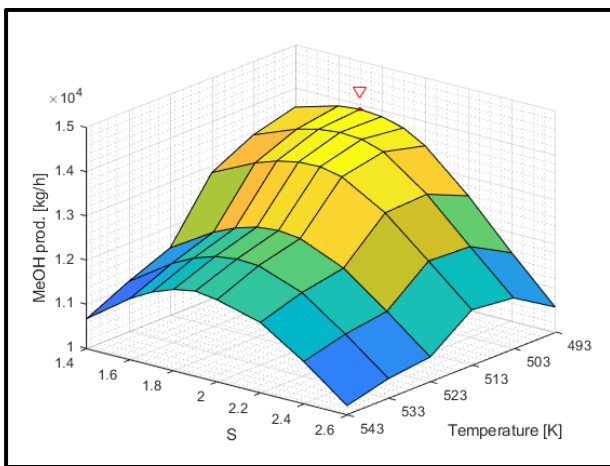

Figure 4.2: Effect of temperature and S value over the methanol production
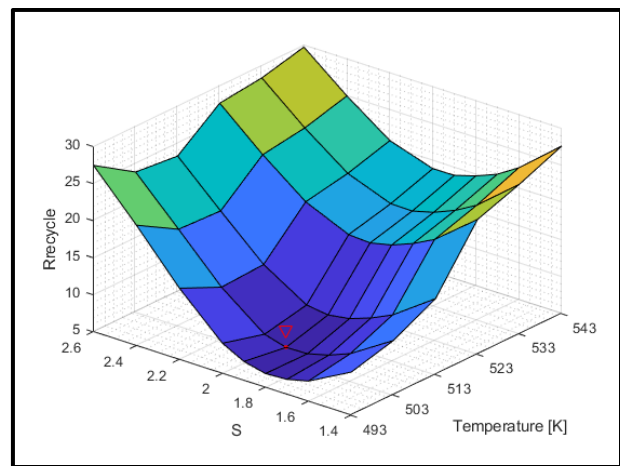

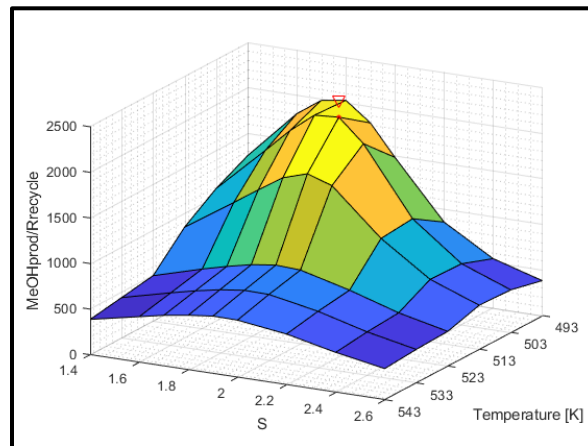*Figure 4.3: Effect of temperature and S value over the Rrecycle*

Figure 4.4: Effect of temperature and S value over the ratio between methanol production and Rrecycle

Both CO and CO_2 conversion per pass are presented in Figure 4.5 and 4.6. It is remarkable that the maximum for CO conversion per pass, which indirectly represent the accumulated reaction

rate for the WGS reaction in the forward direction, is obtained at the same rector's temperature where the ratio between methanol productivity and Rrecycle is maximum (T = 230°C).

The surface plot for the CO2 conversion displays the importance of the temperature in the chemical equilibrium taking place in the reactor, at high enough temperature (T>240°C) the equilibrium from both exothermic reactions are heavily affected, constraining the conversion of CO_2.

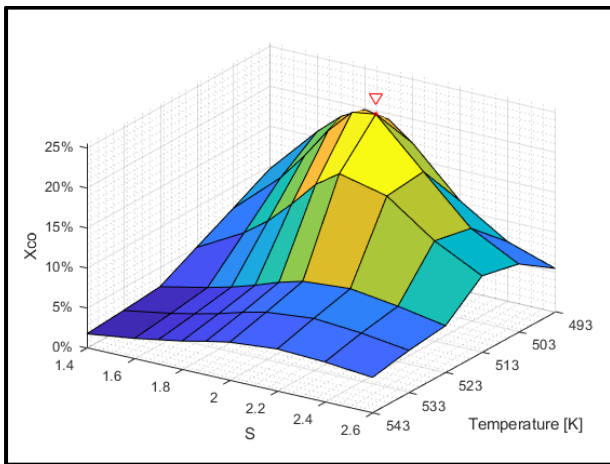*Figure 4.5: Effect of temperature and the S value over the CO conversion per pass*

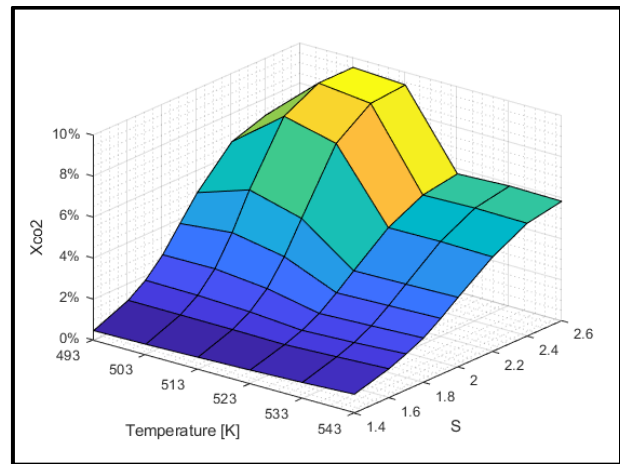*Figure 4.6: Effect of temperature and the S value over the CO_2 conversion per pass*

CO ratio Effect

The following results were obtained for simulation runs with an S value set at 2.0 for the plant feed.

Both methanol production and Rrecycle show a steady slope as CO ratio increases obtaining an extremum for a reactor's temperature of 230°C and a CO ratio plant feed equal to 0.95 (Figure 4.7 and 4.8). At this point, the S and CO ratio at the reactor feed is 2.64 and 0.71 respectively. The ratio between methanol production and Rrecycle (Figure 4.9) makes obvious the presence of a global maximum with a considerable decline on neighbors' configurations.

An important observation is the sudden change at higher CO ratio values observed on both the methanol production and the Rrecycle, this effect is considered to be the ramification of a system with both reaction "stuck" by such a low concentration of reactives. Since both reactions undertake a simultaneous refilling of reactives, even in the presence of a recycle stream, the steady state process cannot reach a high methanol productivity condition.
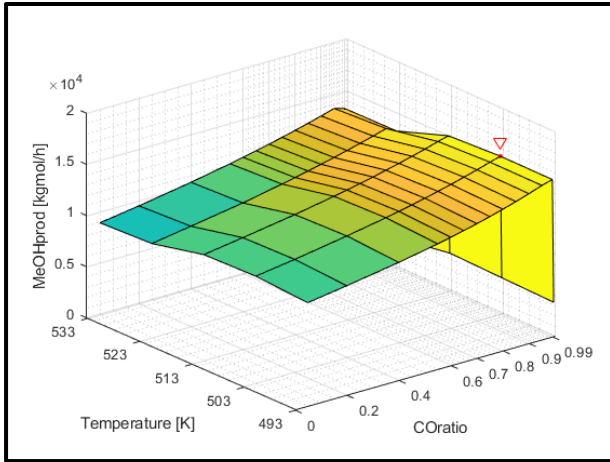
Figure 4.7: Effect of CO ratio and temperature over the methanol production
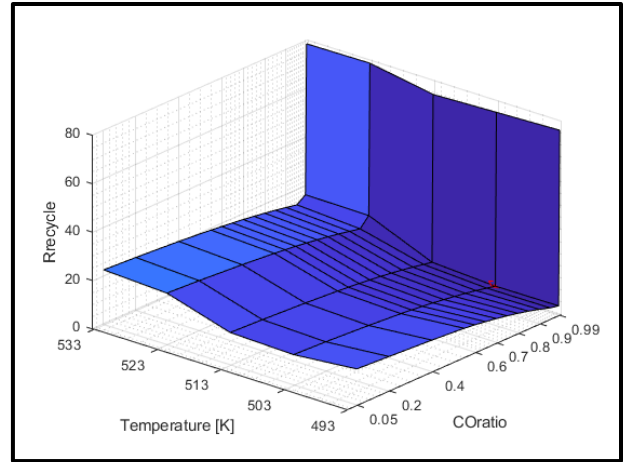
Figure 4.8: Effect of CO ratio and temperature over the Rrecycle
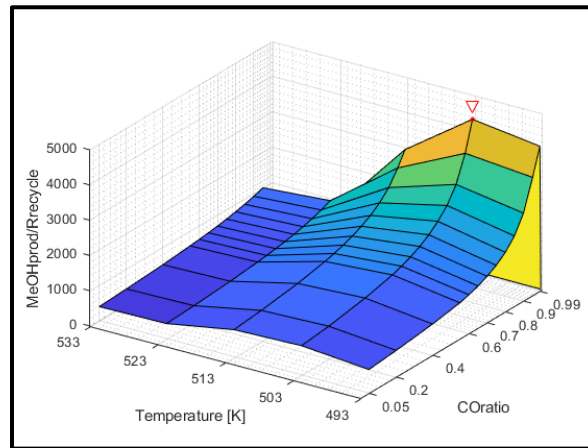
Figure 4.9: Effect of CO ratio and temperature over the ratio between methanol production and Rrecycle

The conversion per pass for CO shows a maximum at the similar CO ratio - temperature configuration (Figure 4.10). For the CO_2 conversion it can be seen that it decreases as CO ratio increases, this is due to the way the conversion is calculated, from the inlet and outlet of the reactor, but at high CO ratio values, the CO is produced inside the reactor by the WGS reaction while simultaneously being consumed by the hydrogenation reaction.

Figure 4.10: Effect of CO ratio and temperature over the CO conversion per pass

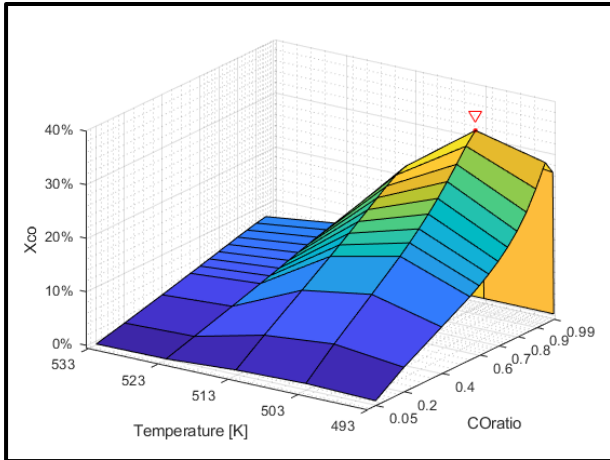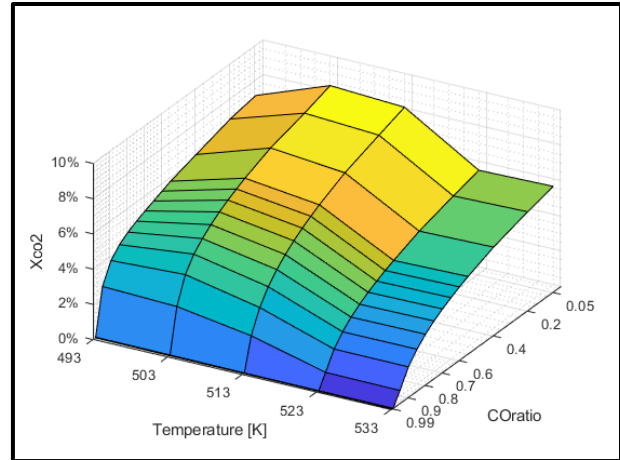*Figure 4.11: Effect of CO ratio and temperature over the CO₂ conversion per pass*

As much as these results shows that a higher CO ratio gives a higher methanol production and lower Rrecycle, the disadvantage is that it will affect negatively the time it takes the plant to reach the steady state. At a higher CO ratio, the hydrogenation is limited by the low amount of CO_2 present at the startup of the plant, but at the same time, the WGS reaction, even with high amount of CO in the feed, does not present a high reaction rate by being limited by the low amount of water in the system, which is expected from the CO_2 hydrogenation. This can be easily countered by adding water to the feed at the startup of the plant.

Catalyst loading Effect

The following results were obtained for simulation runs with a reactor's temperature of 230°C and an CO ratio of 0.75 at the plant's feed.

An important aspect of the reactor design is the amount of catalyst load into the reactor; as observed from previous results, the best reaction scheme for a general case is to have the WGS reaction refilling the CO_2 needed for the hydrogenation reaction. Since from both reactions the WGS reaction is slightly slower, it reaching the chemical equilibrium presents a limit in the maximum conversion per pass that can be reachable, meaning, there exist a critical amount of catalyst loading after which a higher amount will not improve a meaningful increase in methanol production

On Figure 4.12 it is made clear that this catalyst loading critical value is presented at a gas hourly space velocity (GHSV) value of 12.1 [m³/kgCat/h] depicted by a by a solid red line in the plot. A similar situation is proven in Figure 4.13 for the Rrecycle.

As before, the ratio between methanol production and Rrecycle in Figure 4.14 can show a clearer situation. The maximum point is reached at a S value for the plant feed is 1.9 and a GHSV of 2.7 [m³/kgCat/h].
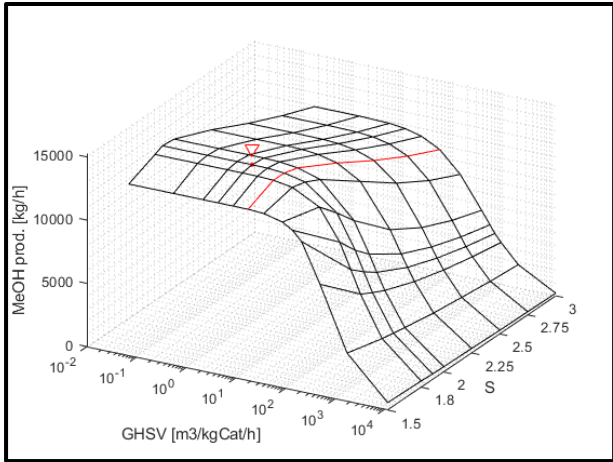
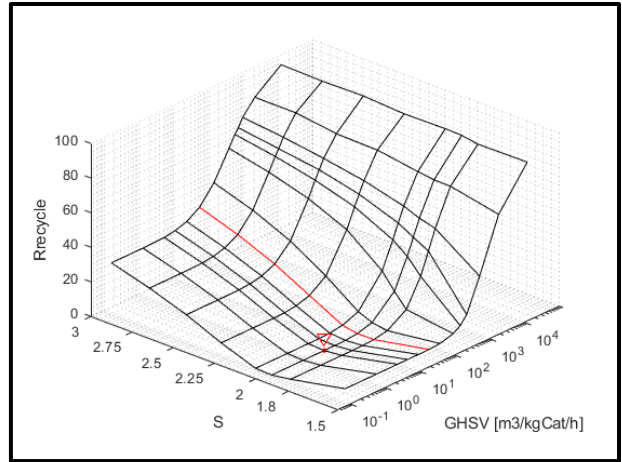Figure 4.12: Effect of GHSV and S value over the methanol production

Figure 4.13: Effect of GHSV and S over the Rrecycle

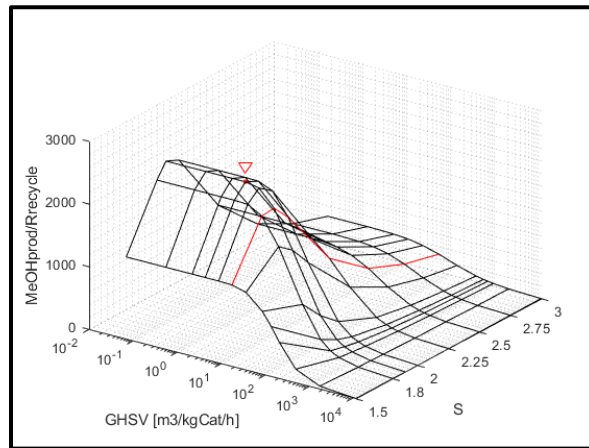

Figure 4.14: Effect of GHSV and S value over the ratio between methanol production and Rrecycle

Conclusions

Methanol presents to be a real alternative to fix the intermittent problem present in renewable energy sources, it can present itself as an energy storage intermediary to the excess of renewable energy available at high producing hours to fewer producing ones. His precursor, identified to be the primal culprit for the greenhouse effect, it the most common by-product in the industry. Hydrogen can be cleanly obtained from water by electrolysis, while its other product, oxygen, can be later used in direct methanol fuel cells converting methanol and oxygen into carbon dioxide, water and electricity.

It is evident the importance of a proper selection of the feed composition to manage the "harmony" between the hydrogenation and the WGS reactions. It was proved that the best configuration is the one that forces the WGS reaction to go forward, producing the reactives needed by the CO_2 hydrogenation while simultaneously consuming the water present as a by-product, both key points in maintaining a favorable equilibrium constant.

The reactor's temperature has a huge impact in the methanol synthesis process, at higher values it favors faster kinetics, but, since both of the reaction involved are exothermic, it negatively affects the equilibrium constant. From these results is observable that a low temperature is preferable, which adds importance to the thermal control system implementation.

Methanol synthesis is recognizable for being a process with an incomplete conversion per pass. Because of this, a recycle stream is used to recover unreacted compounds. It was demonstrated how the feed, reactor, and separation characteristics has an effect in this index affecting the overall capital and operational cost.

References

An, X. *et al.* (2007) 'A Cu/Zn/Al/Zr Fibrous Catalyst that is an Improved CO_2 Hydrogenation to Methanol Catalyst', *Catalysis Letters*. Springer US, 118(3–4), pp. 264–269. doi: 10.1007/s10562-007-9182-x.

Angelo, L. *et al.* (2015) 'Study of CuZnMOx oxides (M = Al, Zr, Ce, CeZr) for the catalytic hydrogenation of CO_2 into methanol', *Comptes Rendus Chimie*. Elsevier Masson, 18(3), pp. 250–260. doi: 10.1016/J.CRCI.2015.01.001.

Arab, S. *et al.* (2014) 'Methanol synthesis from CO_2 and H_2 in multi-tubular fixed-bed reactor and multi-tubular reactor filled with monoliths', *Chemical Engineering Research and Design*. Elsevier, 92(11), pp. 2598–2608. doi: 10.1016/J.CHERD.2014.03.009.

Aresta, M., Dibenedetto, A. and Angelini, A. (2013) 'The changing paradigm in CO_2 utilization', *Journal of CO2 Utilization*. Elsevier, 3–4, pp. 65–73. doi: 10.1016/J.JCOU.2013.08.001.

Audibert, E. and Raineau, A. (1928) 'A Study of the Synthesis of Methanol 1', *Industrial & Engineering Chemistry*. American Chemical Society, 20(10), pp. 1105–1110. doi: 10.1021/ie50226a034.

Avgouropoulos, G. and Ioannides, T. (2003) 'Selective CO oxidation over CuO-CeO2 catalysts prepared via the urea-nitrate combustion method', *Applied Catalysis A: General*, 244(1), pp. 155–167. doi: 10.1016/S0926-860X(02)00558-6.

Bakemeier, H., Laurer, P. and Schroeder, W. (1970) 'ChemInform Abstract: ENTWICKLUNG UND ANWENDUNG EINES MATHEMATISCHEN MODELLS DER METHANOL-SYNTH.', *Chemischer Informationsdienst. Organische Chemie*. John Wiley & Sons, Ltd, 1(20), p. no-no. doi: 10.1002/chin.197020114.

BASF (1913) 'Patent 293787'. Germany.

van Bennekom, J. G. *et al.* (2013) 'Methanol synthesis beyond chemical equilibrium', *Chemical Engineering Science*. Pergamon, 87, pp. 204–208. doi: 10.1016/J.CES.2012.10.013.

Bowker, M. *et al.* (1988) 'The mechanism of methanol synthesis on copper/zinc oxide/alumina catalysts', *Journal of Catalysis*. Academic Press, 109(2), pp. 263–273. doi: 10.1016/0021-9517(88)90209-6.

Bulko, J. B. *et al.* (1979) 'Optical properties and electronic interactions of microcrystalline copper/zinc oxide (Cu/ZnO) catalysts', *The Journal of Physical Chemistry*. American Chemical Society, 83(24), pp. 3118–3122. doi: 10.1021/j100487a011.

Vanden Bussche, K. M. and Froment, G. F. (1996) 'A Steady-State Kinetic Model for Methanol Synthesis and the Water Gas Shift Reaction on a Commercial Cu/ZnO/Al2O3Catalyst', *Journal of Catalysis*. Academic Press, 161(1), pp. 1–10. doi: 10.1006/JCAT.1996.0156.

Buzzi-Ferraris, G. and Manenti, F. (2012) 'BzzMath: Library Overview and Recent Advances in Numerical Methods', *Computer Aided Chemical Engineering*. Elsevier, 30, pp. 1312–1316. doi: 10.1016/B978-0-444-59520-1.50121-4.

Centi, G. and Perathoner, S. (2009) 'Opportunities and prospects in the chemical recycling of carbon dioxide to fuels', *Catalysis Today*. Elsevier, 148(3–4), pp. 191–205. doi: 10.1016/J.CATTOD.2009.07.075.

Chapple, F. H. and Stone, F. S. (1964) 'The optical properties of the cupric ion in oxide crystal fields of differing symmetries', in *Proc. Br. Ceram. Soc*, pp. 45–58.

Chinchen, G. C. *et al.* (1988) 'Synthesis of Methanol: Part 1. Catalysts and Kinetics', *Applied Catalysis*. Elsevier, 36, pp. 1–65. doi: 10.1016/S0166-9834(00)80103-7.

Chinchen, G. C., Waugh, K. C. and Whan, D. A. (1986) 'The activity and state of the copper surface in methanol synthesis catalysts', *Applied Catalysis*. Elsevier, 25(1–2), pp. 101–107. doi: 10.1016/S0166-9834(00)81226-9.

Dalena, F. *et al.* (2018) 'Methanol Production and Applications: An Overview', *Methanol*. Elsevier, pp. 3–28. doi: 10.1016/B978-0-444-63903-5.00001-7.

Data and Statistics - IRENA REsource (no date). Available at: http://resourceirena.irena.org/gateway/dashboard/?topic=4&subTopic=16 (Accessed: 15 February 2020).

Demirci, U. B. (2007) 'Direct liquid-feed fuel cells: Thermodynamic and environmental concerns', *Journal of Power Sources*. Elsevier, 169(2), pp. 239–246. doi: 10.1016/J.JPOWSOUR.2007.03.050.

Dybkjær, I. *et al.* (2006) 'Tecnologie per la produzione di metanolo', in *Enciclopedia degli Idrocarburi*. Rome.

Effective Carbon Rates 2018 (2018). OECD. doi: 10.1787/9789264305304-en.

Ernst, K.-H. *et al.* (1991) 'The titration of oxygen adatoms by H2 from the Cs-promoted Cu(110) surface', *Surface Science*. North-Holland, 259(1–2), pp. 18–25. doi: 10.1016/0039-6028(91)90520-3.

Fischer, F. and Hans, T. (1923) 'Über die reduktion des kohlenstoffdioxid zu methan betonkontakt unter Druck', *Brennstoff-Chemie*, 4, pp. 193–197.

Frolich, P. K. *et al.* (1929) 'Studies of copper catalyst prepared from precipitated hydroxide. II comparison of sodium hydroxide and ammonia as a precipitating agent', *Journal of the American Chemical Society*. American Chemical Society, 51(1), pp. 187–193. doi: 10.1021/ja01376a023.

Froment, G. F., De Wilde, J. and Bischoff, K. B. (2011) *Chemical reactor analysis and design*. 3rd edn. Wiley.

Fujita, S. *et al.* (1992) 'Methanol synthesis from carbon dioxide at atmospheric pressure over Cu/ZnO catalyst. Role of methoxide species formed on ZnO support', *Catalysis Letters*. Baltzer Science Publishers, Baarn/Kluwer Academic Publishers, 13(4), pp. 349–358. doi: 10.1007/BF00765037.

Fujitani, T. *et al.* (1994) 'The role of metal oxides in promoting a copper catalyst for methanol synthesis', *Catalysis Letters*. Baltzer Science Publishers, Baarn/Kluwer Academic Publishers, 25(3–4), pp. 271–276. doi: 10.1007/BF00816307.

Ganesh, I. (2014) 'Conversion of carbon dioxide into methanol – a potential liquid fuel: Fundamental challenges and opportunities (a review)', *Renewable and Sustainable Energy Reviews*. Pergamon, 31, pp. 221–257. doi: 10.1016/J.RSER.2013.11.045.

Graaf, G. H. *et al.* (1986) 'Chemical equilibria in methanol synthesis', *Chemical Engineering Science*. Pergamon, 41(11), pp. 2883–2890. doi: 10.1016/0009-2509(86)80019-7.

Graaf, G. H., Stamhuis, E. J. and Beenackers, A. A. C. M. (1988) 'Kinetics of low-pressure methanol synthesis', *Chemical Engineering Science*. Pergamon, 43(12), pp. 3185–3195. doi: 10.1016/0009-2509(88)85127-3.

Grabow, L. C. and Mavrikakis, M. (2011) 'Mechanism of Methanol Synthesis on Cu through CO 2 and CO Hydrogenation', *ACS Catalysis*. American Chemical Society, 1(4), pp. 365–384. doi: 10.1021/cs200055d.

Gumber, S. and Gurumoorthy, A. V. P. (2018) 'Methanol Economy Versus Hydrogen Economy', *Methanol*. Elsevier, pp. 661–674. doi: 10.1016/B978-0-444-63903-5.00025-X.

Herman, R. G. *et al.* (1979) 'Catalytic synthesis of methanol from carbon monoxide/hydrogen. I. Phase composition, electronic properties, and activities of the copper/zinc oxide/M2O3 catalysts', *Chemischer Informationsdienst*. John Wiley & Sons, Ltd, 10(25), p. no-no. doi: 10.1002/chin.197925142.

Hu, L. H. *et al.* (2008) 'Study of the Characteristics of Methanol Synthesis in a Recirculation Slurry Reactor – A Novel Three-Phase Synthesis Reactor', *Chemical Engineering & Technology*. John Wiley & Sons, Ltd, 31(1), pp. 33–37. doi: 10.1002/ceat.200700081.

Hüttig, G. F. and Goerk, H. (1937) 'Zinkoxyde, welche durch thermische Zersetzung verschiedener komplexer Zinkoxalate entstanden sind, als Katalysatoren des Methanolzerfalles [Aktive Oxyde. 106. Mitteilung]', *Zeitschrift für anorganische und allgemeine Chemie*. John Wiley & Sons, Ltd, 231(3), pp. 249–263. doi: 10.1002/zaac.19372310304.

Hüttig, G. F., Kostelitz, O. and Fehèr, I. (1931) 'Über die Beziehungen zwischen der Vorgeschichte des Zinkoxydes und seinem katalytischen Wirkungsgrad bei dem Methanolzerfall', *Zeitschrift für anorganische und allgemeine Chemie*. John Wiley & Sons, Ltd, 198(1), pp. 206–218. doi: 10.1002/zaac.19311980120.

Ipatiev, V. and Dolgov, B. (1931) 'No Title', *Journal of Industrial and Engineering Chemistry*, 8, p. 825.

Ivannikov, P., Frost, A. and Shapiro, M. (1934) 'No Title', *Comptes rendus de l'Académie des Sciences*, (1), p. 49.

Kanai, Y. *et al.* (1994) 'Evidence for the migration of ZnOx in a Cu/ZnO methanol synthesis catalyst', *Catalysis Letters*. Baltzer Science Publishers, Baarn/Kluwer Academic Publishers, 27(1–2), pp. 67–78. doi: 10.1007/BF00806979.

Kanai, Y. *et al.* (1996) 'The synergy between Cu and ZnO in methanol synthesis catalysts', *Catalysis Letters*. Baltzer Science Publishers, Baarn/Kluwer Academic Publishers, 38(3–4), pp. 157–163. doi: 10.1007/BF00806562.

Kattel, S. *et al.* (2017) 'Active sites for CO2 hydrogenation to methanol on Cu/ZnO catalysts.', *Science (New York, N.Y.)*. American Association for the Advancement of Science, 355(6331), pp. 1296–1299. doi: 10.1126/science.aal3573.

Kiss, A. A. *et al.* (2016) 'Novel efficient process for methanol synthesis by CO2 hydrogenation', *Chemical Engineering Journal*. Elsevier, 284, pp. 260–269. doi: 10.1016/j.cej.2015.08.101.

Klier, K. *et al.* (1982) 'Catalytic synthesis of methanol from COH2: IV. The effects of carbon dioxide', *Journal of Catalysis*. Academic Press, 74(2), pp. 343–360. doi: 10.1016/0021-9517(82)90040-9.

Klier, K. (1982) 'Methanol Synthesis', *Advances in Catalysis*. Academic Press, 31, pp. 243–313. doi: 10.1016/S0360-0564(08)60455-1.

Kostelitz, O. and Hensinger (1939) 'No Title', *Chimie & industrie*, 40, p. 757.

Kubota, T. *et al.* (2001) 'Kinetic study of methanol synthesis from carbon dioxide and hydrogen', *Applied Organometallic Chemistry*. John Wiley & Sons, Ltd, 15(2), pp. 121–126. doi: 10.1002/1099-0739(200102)15:2<121::AID-AOC106>3.0.CO;2-3.

Kuld, S. *et al.* (2016) 'Quantifying the promotion of Cu catalysts by ZnO for methanol synthesis.', *Science (New York, N.Y.)*. American Association for the Advancement of Science, 352(6288), pp. 969–74. doi: 10.1126/science.aaf0718.

Kung, H. H. (1980) 'Methanol Synthesis', *Catalysis Reviews*. Taylor & Francis Group, 22(2), pp. 235–259. doi: 10.1080/03602458008066535.

Lamy, C. *et al.* (2002) 'Recent advances in the development of direct alcohol fuel cells (DAFC)', *Journal of Power Sources*. Elsevier, 105(2), pp. 283–296. doi: 10.1016/S0378-7753(01)00954-5.

Lee, S. and Sardesai, A. (2005) 'Liquid phase methanol and dimethyl ether synthesis from syngas', *Topics in Catalysis*. Kluwer Academic Publishers-Plenum Publishers, 32(3–4), pp. 197–207. doi: 10.1007/s11244-005-2891-8.

Leonov, V. E. *et al.* (1973) 'Kinetik der methanol-synthese an einem tieftemperatur-katalysator', *Chemischer Informationsdienst*. John Wiley & Sons, Ltd, 4(49), p. no-no. doi: 10.1002/chin.197349216.

Li, X. and Faghri, A. (2013) 'Review and advances of direct methanol fuel cells (DMFCs) part I: Design, fabrication, and testing with high concentration methanol solutions', *Journal of Power Sources*. Elsevier, 226, pp. 223–240. doi: 10.1016/j.jpowsour.2012.10.061.

Lim, H.-W. *et al.* (2009) 'Modeling of the Kinetics for Methanol Synthesis using Cu/ZnO/Al 2 O 3 /ZrO 2 Catalyst: Influence of Carbon Dioxide during Hydrogenation', *Industrial & Engineering Chemistry Research*. American Chemical Society, 48(23), pp. 10448–10455. doi: 10.1021/ie901081f.

Liu, X.-M. *et al.* (2003) 'Recent Advances in Catalysts for Methanol Synthesis via Hydrogenation of CO and CO2', *Industrial & Engineering Chemistry Research*. American Chemical Society, 42(25), pp. 6518–6530. doi: 10.1021/IE020979S.

Lu, G. Q., Liu, F. Q. and Wang, C. Y. (2005) 'Water transport through Nafion 112 membrane in DMFCs', *Electrochemical and Solid-State Letters*. IOP Publishing, 8(1), p. A1. doi: 10.1149/1.1825312.

Malinovskaya, O. A. *et al.* (1987) 'Synthesis of methanol on Cu-based catalyst: Kinetic model', *Reaction Kinetics and Catalysis Letters*. Kluwer Academic Publishers, 34(1), pp. 87–92. doi: 10.1007/BF02069206.

Marek, L. F. and Hahn, D. A. (1933) 'Catalytic Oxidation of Organic Compounds in the Vapor Phase.', *The Journal of Physical Chemistry*. American Chemical Society, 37(5), pp. 657–657. doi: 10.1021/j150347a012.

Matsumura, Y. and Ishibe, H. (2009) 'High temperature steam reforming of methanol over Cu/ZnO/ZrO2 catalysts', *Applied Catalysis B: Environmental*. Elsevier, 91(1–2), pp. 524–532. doi: 10.1016/J.APCATB.2009.06.023.

McNeil, M. A., Schack, C. J. and Rinker, R. G. (1989) 'Methanol synthesis from hydrogen, carbon monoxide and carbon dioxide over a CuO/ZnO/Al2O3 catalyst: II. Development of a phenomenological rate expression', *Applied Catalysis*. Elsevier, 50(1), pp. 265–285. doi: 10.1016/S0166-9834(00)80841-6.

Mears, D. E. (1971) 'Tests for Transport Limitations in Experimental Catalytic Reactors', *Industrial & Engineering Chemistry Process Design and Development*. American Chemical Society, 10(4), pp. 541–547. doi: 10.1021/i260040a020.

Mehta, S. *et al.* (1979) 'Catalytic synthesis of methanol from COH2: II. Electron microscopy (TEM, STEM, microdiffraction, and energy dispersive analysis) of the CuZnO and Cu/ZnO/Cr2O3 catalysts', *Journal of Catalysis*. Academic Press, 57(3), pp. 339–360. doi: 10.1016/0021-9517(79)90001-0.

Millar, G. J., Rochester, C. H. and Waugh, K. C. (1991) 'Infrared study of methyl formate and formaldehyde adsorption on reduced and oxidised silica-supported copper catalysts', *Journal of the Chemical Society, Faraday Transactions*, 87(17), pp. 2785–2793. doi: 10.1039/FT9918702785.

Mittasch, A. and Pier, M. (1925) 'Synthetic Manufacture of Methanol.', *Industrial & Engineering Chemistry*. American Chemical Society, 17(9), pp. 981–982. doi: 10.1021/ie50189a045.

Mochalin, Lin and Rozovskii (1984) 'Kinetic-model of the process of methanol synthesis on the snm-1 catalyst', *Khimicheskaya Promyshlennost*, 1(11).

Molstad, M. C. and Dodge, B. F. (1935) 'Zinc Oxide–Chromium Oxide Catalysts for Methanol Synthesis', *Industrial & Engineering Chemistry*. American Chemical Society, 27(2), pp. 134–140. doi: 10.1021/ie50302a005.

Nakamura, J., Campbell, J. M. and Campbell, C. T. (1990) 'Kinetics and mechanism of the water-gas shift reaction catalysed by the clean and Cs-promoted Cu(110) surface: a comparison with Cu(111)', *Journal of the Chemical Society, Faraday Transactions*. The Royal Society of Chemistry, 86(15), p. 2725. doi: 10.1039/ft9908602725.

Nakamura, J., Choi, Y. and Fujitani, T. (2003) 'On the Issue of the Active Site and the Role of ZnO in Cu/ZnO Methanol Synthesis Catalysts', *Topics in Catalysis*, 22(3), pp. 277–285. doi: 10.1023/A:1023588322846.

Natta, G. (1955) 'Synthesis of Methanol', in, pp. 349–411.

Natta, G. and Corradini, P. (1952) 'Influence des reactions a l'etat solide sur l'active des catalyseurs a base d'oxyde de zinc', in *International symposium on the reactivity of solids*.

Neophytides, S. G., Marchi, A. J. and Froment, G. F. (1992) 'Methanol synthesis by means of diffuse reflectance infrared Fourier transform and temperature-programmed reaction spectroscopy', *Applied Catalysis A: General*. Elsevier, 86(1), pp. 45–64. doi: 10.1016/0926-860X(92)80041-A.

Ng, K. L., Chadwick, D. and Toseland, B. A. (1999) 'Kinetics and modelling of dimethyl ether synthesis from synthesis gas', *Chemical Engineering Science*. Pergamon, 54(15–16), pp. 3587–3592. doi: 10.1016/S0009-2509(98)00514-4.

Olah, G. A. (2005) 'Beyond Oil and Gas: The Methanol Economy', *Angewandte Chemie International Edition*. John Wiley & Sons, Ltd, 44(18), pp. 2636–2639. doi: 10.1002/anie.200462121.

Park, N., Park, M.-J., *et al.* (2014) 'Kinetic modeling of methanol synthesis over commercial catalysts based on three-site adsorption', *Fuel Processing Technology*. Elsevier, 125, pp. 139–147. doi: 10.1016/J.FUPROC.2014.03.041.

Park, N., Kim, J. R., *et al.* (2014) 'Modeling of a pilot-scale fixed-bed reactor for iron-based Fischer-Tropsch synthesis: Two-dimensional approach for optimal tube diameter', *Fuel*, 122, pp. 229–235. doi: 10.1016/j.fuel.2014.01.044.

Peppley, B. A. *et al.* (1999) 'Methanol–steam reforming on Cu/ZnO/Al2O3 catalysts. Part 2. A comprehensive kinetic model', *Applied Catalysis A: General*. Elsevier, 179(1–2), pp. 31–49. doi: 10.1016/S0926-860X(98)00299-3.

Pinto, A. (1983) 'Method for Producing Methanol and Ammonia'. United States of America.

Plotnikov, V. and Ivanov, P. (1934) 'No Title', *Allukrain. Akad. Sci. Mem. Inst. Chem.*, 1(127).

Qian, W. *et al.* (2006) 'Architecture for portable direct liquid fuel cells', *Journal of Power Sources*. Elsevier, 154(1), pp. 202–213. doi: 10.1016/J.JPOWSOUR.2005.12.019.

Rivera-Tinoco, R. *et al.* (2016) 'Investigation of power-to-methanol processes coupling electrolytic hydrogen

production and catalytic CO2 reduction', *International Journal of Hydrogen Energy*. Pergamon, 41(8), pp. 4546–4559. doi: 10.1016/J.IJHYDENE.2016.01.059.

Rozovskii, A. Y. (1989) 'Modern problems in the synthesis of methanol', *Russian Chemical Reviews*, 58(1), pp. 41–56. doi: 10.1070/RC1989v058n01ABEH003425.

Sá, S. *et al.* (2010) 'Catalysts for methanol steam reforming—A review', *Applied Catalysis B: Environmental*. Elsevier, 99(1–2), pp. 43–57. doi: 10.1016/J.APCATB.2010.06.015.

Schack, C. J., McNeil, M. A. and Rinker, R. G. (1989) 'Methanol synthesis from hydrogen, carbon monoxide, and carbon dioxide over a CuO/ZnO/Al2O3 catalyst: I. Steady-state kinetics experiments', *Applied Catalysis*. Elsevier, 50(1), pp. 247–263. doi: 10.1016/S0166-9834(00)80840-4.

Schermuly, O. and Luft, G. (1977) 'Untersuchung der Niederdruck-Methanolsynthese im Treibstrahlreaktor', *Chemie Ingenieur Technik*. John Wiley & Sons, Ltd, 49(11), pp. 907–907. doi: 10.1002/cite.330491111.

Schiavello, M., Pepe, F. and De Rossi, S. (1974) 'The Catalytic Activity of Copper Ions in Copper Oxides and in their Solid Solutions with ZnO and MgO for the Decomposition of N 2 O', *Zeitschrift für Physikalische Chemie*. Akademische Verlagsgesellschaft, 92(1–3), pp. 109–124. doi: 10.1524/zpch.1974.92.1-3.109.

Seyfert, W. and Luft, G. (1985) 'Untersuchungen zur Methanol-Synthese im Mitteldruckbereich', *Chemie Ingenieur Technik*. John Wiley & Sons, Ltd, 57(5), pp. 482–483. doi: 10.1002/cite.330570526.

Shamsul, N. S. *et al.* (2014) 'An overview on the production of bio-methanol as potential renewable energy', *Renewable and Sustainable Energy Reviews*. Elsevier Ltd, pp. 578–588. doi: 10.1016/j.rser.2014.02.024.

Soave, G. (1972) 'Equilibrium constants from a modified Redlich-Kwong equation of state', *Chemical Engineering Science*. Pergamon, 27(6), pp. 1197–1203. doi: 10.1016/0009-2509(72)80096-4.

Specht, M. and Bandi, A. (1999) *The 'methanol cycle' - sustainable supply of liquid fuels*. Cologne. Available at: https://www.osti.gov/etdeweb/biblio/20010964.

Styhr Petersen, H. J. (1972) 'Low Temperature Methanol Synthesis'. United Kingdom.

Szima, S. and Cormos, C. C. (2018) 'Improving methanol synthesis from carbon-free H2 and captured CO2: A techno-economic and environmental evaluation', *Journal of CO2 Utilization*. Elsevier Ltd, 24, pp. 555–563. doi: 10.1016/j.jcou.2018.02.007.

Tanaka, N. (2008) *Prospects for CO2 capture and storage*. IEA Publications.

Veltistova, M., Dolgov, B. and Karpov, A. (1934) 'No Title', *Journal of Indutrial and Engineering Chemistry*, 9(24).

Villa, P. *et al.* (1985) 'Synthesis of alcohols from carbon oxides and hydrogen. 1. Kinetics of the low-pressure methanol synthesis', *Industrial & Engineering Chemistry Process Design and Development*. American Chemical Society, 24(1), pp. 12–19. doi: 10.1021/i200028a003.

Wachs, I. E. and Madix, R. J. (1978) 'The selective oxidation of CH3OH to H2CO on a copper(110) catalyst', *Journal of Catalysis*, 53(2), pp. 208–227. doi: 10.1016/0021-9517(78)90068-4.

Wee, J. H. (2007) 'A feasibility study on direct methanol fuel cells for laptop computers based on a cost comparison with lithium-ion batteries', *Journal of Power Sources*. Elsevier, pp. 424–436. doi: 10.1016/j.jpowsour.2007.04.084.

Wilhelm, D. . *et al.* (2001) 'Syngas production for gas-to-liquids applications: technologies, issues and outlook', *Fuel Processing Technology*. Elsevier, 71(1–3), pp. 139–148. doi: 10.1016/S0378-3820(01)00140-0.

Yong, S. T. *et al.* (2013) 'Review of methanol reforming-Cu-based catalysts, surface reaction mechanisms, and reaction schemes', *International Journal of Hydrogen Energy*. Pergamon, 38(22), pp. 9541–9552. doi: 10.1016/J.IJHYDENE.2013.03.023.

Young, L. C. and Finlayson, B. A. (1973) 'Axial Dispersion in Nonisothermal Packed Bed Chemical Reactors', *Industrial & Engineering Chemistry Fundamentals*. American Chemical Society, 12(4), pp. 412–422. doi: 10.1021/i160048a004.

Zhen, X. and Wang, Y. (2015) 'An overview of methanol as an internal combustion engine fuel', *Renewable and Sustainable Energy Reviews*. Pergamon, 52, pp. 477–493. doi: 10.1016/J.RSER.2015.07.083.

"